ERASMUS UNIVERSITY ROTTERDAM

Erasmus School of Economics

Bachelor Thesis BSc^2 in Econometrics and Economics

Comparing asymmetric volatility spillover models: A study between the crude oil market and international stock markets

Peter Jan Snijders

473330

Abstract

In this paper, I examine whether or not incorporating the different stylized facts associated with volatility provides better insights in asymmetric volatility spillovers between the oil market and three global stock markets. This is done by using a VAR and a VHAR model, which is able to capture the stylized facts, in combination with the DAG technique. Both models show that over the sample period, bad volatility spillovers dominate the markets which implies a pessimistic market sentiment and the presence of uninformed traders on the market. Moreover, during and after the global financial crisis volatility spillovers from the oil market to the stock markets are predominantly positive implying that oil futures can be used as a hedge against such crises. Furthermore, the results show that asymmetries in volatility spillovers are highly influenced by the economic and political events between 2002 and 2014. However, incorporating the stylized facts associated with volatility by means of a VHAR model does not lead to new useful insights.

Supervisor: M. D. Zaharieva

Second assessor: T. van der Zwan

July 20, 2021

Contents

1 Introduction

The financial and economic turbulence during the financial crisis of 2007-2008 has made it apparent once again that the global markets are highly interdependent. The subprime mortgage fears that began in the United States and peaked with the fall of Lehman Brothers in September 2008 spread across the markets, resulting in a global financial crisis, whose ramifications are the United States and European sovereign debt crises (Fengler & Gisler, 2015). By February 2009, stock markets had declined over 40%, the crude oil price by more than 60% and implied volatilities of equities and oil spiked to crisis levels. According to Fengler and Gisler (2015), crises like these generally come along with a regular pattern where the most notable signal of this pattern is the significant surge in volatility, reflecting the increased uncertainty in the markets. Moreover, volatility tends to spill over between markets. Especially relevant are the spillovers between the crude oil market and stock markets, as crude oil has been proven to have a significant influence on the global economy as well as financial markets (Chen et al., 1986; Ji et al., 2018; Wen et al., 2012).

So, what effects do shifts in the oil market's and stock markets' volatility have on each other? Decomposing the overall volatility into two separate components, 'good' volatility and 'bad' volatility, yields a much simpler answer to this question (Segal et al., 2015). On the one hand, a market's return volatility may be higher because better diversification opportunities and more productive use of inputs allow investors to take on more risk, resulting in increased market growth (Acemoglu & Zilibotti, 1997; Obstfeld, 1994). On the other hand, a market's return volatility may be higher due to risks that are hard to eliminate like political threats, pandemics or natural disasters (Bartram et al., 2012; Corbet et al., 2021; Kliesen & Mill, 1994). In the former case, high volatility is beneficial because it results from positive shocks that enable markets to function more efficiently. However, in the latter case, high volatility destabilizes and stagnates the market (Wang & Wu, 2018).

Similar to Wang and Wu (2018), I explore the asymmetries in volatility spillovers between the oil market and three global stock markets that emerge due to the aforementioned good and bad volatility. Wang and Wu (2018) do this by constructing volatility spillovers with vector autoregressive (VAR) models. However, a disadvantage of this approach and many other standard volatility models, such as generalized autoregressive conditional heteroskedasticity (GARCH) models, is that they are not able to capture the different stylized facts associated with financial time series. For example, these models are unable to take into account the stylized fact that the autocorrelations of absolute and squared returns exhibit long-term persistence, even months after (Corsi, 2009). Additionally, the probability density functions of returns exhibit fat tails that take on different shapes depending on the time scale considered (e.g. daily returns versus weekly returns). As the time scale increases, the probability distributions of returns show a slow and steady convergence to the normal distribution (Corsi, 2009). The VAR model is unable to capture all these stylized facts.

In this paper, I therefore examine whether or not taking into account the stylized facts of volatility provides a better insight in the asymmetric volatility spillovers between the crude oil and three global stock markets (Europe, Japan and the United States) than when using the VAR model approach by Wang and Wu (2018). The analysis is performed by using the aforementioned VAR model and the multivariate extension of the heterogeneous autoregressive (VHAR) model proposed by Corsi (2009), which is able to capture the aforementioned stylized facts associated with volatility. The VAR and VHAR models are used in a refined structural framework in combination with the DAG technique. Then, based on the DAG and structural VAR and VHAR results, the static and dynamic characteristics of asymmetric volatility spillovers are examined using forecast error variance decompositions and volatility spillover indices that are based on the ones introduced by Diebold and Yilmaz (2014), which capture the transmission of volatility from and to markets.

The main findings of this paper show that both models indicate bad volatility spillovers dominate the market, which implies that a pessimistic market sentiment dominates between 2002 and 2015. Moreover, this also indicates that the majority of the market is dominated by uninformed traders who tend to raise volatility. Prominent bidirectional positive spillovers between the oil market and the other markets were found during and after the global financial crisis, indicating that oil futures can be used as a hedge against financial crises in an investor's portfolio. However, incorporating the stylized facts associated with volatility using the VHAR model did not provide a better insight into the asymmetric volatility spillovers as the results found are inconsistent with previous research.

The findings of this paper have important implications for portfolio diversification strategies and risk valuation as it shows whether or not a portfolio is well balanced in terms of good and bad volatility spillovers. If not, investors can lower risks and increase opportunities of their portfolio by decreasing the portfolio weight of bad volatility stocks and increasing the portfolio weight of good volatility stocks. Moreover, this paper adds to the existing literature by being the first to compare the VAR model with a VHAR model and by using a VHAR model in combination with the DAG technique. Previous research mainly used the Cholesky decomposition to identify the system.

The paper is organized as follows. Section 2 provides a more elaborate literature review on the research topic. The data set is described in Section 3. Section 4 details the methods used in modelling the volatility dynamics, volatility spillover indices and model diagnostics. The empirical results are presented and discussed in Section 5. Finally, Section 6 concludes the research and limitations and suggestions for future research are given in Section 7.

2 Literature

In the 2000s the crude oil market experienced extreme price fluctuations. Such price fluctuations are not without consequences as crude oil has been proven to have a major impact on the economy and stock markets (Hamilton, 1983; Kilian & Park, 2009). Consequently, volatility spillovers between the oil and stock markets are crucial for energy policymakers, energy risk management, market participants and portfolio diversification (Xu et al., 2019). As a result, this connection between the oil and stock markets has drawn increased attention around the world in the scientific literature.

For example, in Middle Eastern and North African countries, Maghyereh and Awartani (2016) and Malik and Hammoudeh (2007) find significant volatility spillovers from the oil market to stock markets and not the other way around. The only exception is Saudi Arabia, where significant spillovers are found from the Saudi market to the oil market. Arouri et al. (2011) find significant volatility spillovers between the oil market and stock markets in the United States and Europe. However, they find that in Europe the spillovers are usually unidirectional from the oil market to the stock markets whereas in the United States, spillovers are bidirectional. Bouri (2015) examines the role oil price volatility has on predicting stock market volatility in two small oil-importing countries neighbouring oil-exporting countries. Significant unidirectional volatility spillovers from the oil market to the Jordan stock market were found whereas volatility spillovers between the oil market and Lebanese stock market were insignificant. Furthermore, Maghyereh et al. (2016) examine the directional connectedness between the oil market and 11 major international stock markets. They find that the bulk of volatility spillovers is largely dominated by spillovers from the oil market to stock markets and not vice versa. Hence, overall the direction of volatility spillovers between oil and stock markets seems to be an open question.

This is not surprising as early literature mainly focused on return spillovers between the oil and stock markets, instead of volatility spillovers. The conventional VAR or vector correction error models (VECM) were the common econometric methodologies applied to examine the return spillovers between the oil and stock markets (Wang & Wu, 2018). Huang et al. (1996), for example, investigate the relationship between U.S. stock returns and oil futures returns with a VAR model.

They discover that oil futures returns are uncorrelated with U.S. stock market returns, except in the case of individual oil companies' returns. Maghyereh (2006) examines the relationship between oil price returns and stock market returns in 22 emerging economies. He finds that, contrary to previous research on return spillovers in developed economies, oil price shocks do not have a significant effect on stock market index returns in emerging economies. To analyze the long-run relationship between the crude oil market and international stock markets, Miller and Ratti (2009) use a VECM over a period of about 38 years. They find that over the long-run, stock market returns decrease (increase) as the oil price increases (decreases).

Furthermore, most research that addresses the issue of volatility spillovers between oil and stock markets employs the widely used econometric methodologies of multivariate GARCH-type models (Xu et al., 2019). For example, Hammoudeh et al. (2010) use GARCH models to account for asymmetric shocks caused by world, country, and sector-specific variables on stock return volatility of 27 U.S. sectors in the short- and long-run. Filis et al. (2011) and Guesmi and Fattoum (2014) examine the dynamic volatility spillovers between oil prices and both oil-exporting and oil-importing countries using a multivariate DCC-GARCH-GJR. Filis et al. (2011) find that the conditional volatility of oil and stock prices does not differ for both oil-exporting and oil-importing countries. Moreover, they show that aggregate oil demand shocks have a much larger influence on volatility spillovers than aggregate oil supply shocks that result from the OPEC reducing their production. Both Filis et al. (2011) and Guesmi and Fattoum (2014) find that the oil market cannot be considered a strong 'safe haven' for insurance against stock market losses during times of uncertainty.

However, standard volatility models, such as the GARCH models described above, lack the ability to quantify volatility spillovers (Baruník et al., 2016). Therefore, Diebold and Yilmaz (2009) developed new measures based on forecast error variance decompositions in a VAR framework to quantify the extent of volatility spillovers across markets, overcoming the limitations of the previous literature (Wang & Wu, 2018). Furthermore, Diebold and Yilmaz (2012) improve this technique by introducing volatility spillover measures that are able to dynamically and quantitatively measure the directional volatility spillovers. In other words, it not only shows the volatility spillover's direction, but also the magnitude of the directional volatility spillover between any two markets (Wang & Wu, 2018). Additionally, according to Diebold and Yilmaz (2012) it avoids the contentious issues associated with the existence and definition of 'contagion'. The past decade a significant number of studies have used Diebold and Yilmaz's (2009, 2012) volatility spillover directional measures to analyse dynamic spillovers in various financial markets.

Nonetheless, both of these volatility spillovers have their disadvantages. First of all, Diebold and Yilmaz's (2009) spillover measure adopts the popular Cholesky decomposition in order to identify the VARs and thus, the resulting variance decompositions can be dependent on the variable ordering (Diebold & Yilmaz, 2012). Diebold and Yilmaz (2012) overcome this problem by proposing a spillover measure that is constructed in a generalized VAR framework so that variance decompositions are invariant to the variable ordering. However, Diebold and Yilmaz's (2012) spillover measure is still not capable of letting the data speak for itself in order to uncover the network of contemporaneous causal relations among variables (Yang & Zhou, 2017).

To overcome this problem, Yang and Zhou (2017) were one of the first to use the directed acyclic graph (DAG) technique in combination with a spillover index similar to the one used by Diebold and Yilmaz (2009, 2012). Using the DAG technique is advantageous because according to Bessler and Yang (2003), the DAG technique is able to provide a structure of causality among financial markets in a contemporaneous time and therefore let the data speak for itself. Yang and Zhou (2017) examine volatility spillovers between commodities, international stock indices and U.S. Treasury bonds. They find that the stock market in the United States is at the center of the international volatility spillover network, and that volatility spillovers from the U.S. stock market to other stock markets have increased since 2008. Similarly, Wang and Wu (2018) use the DAG technique to investigate asymmetric volatility spillovers between oil and global stock markets in a VAR framework, finding that bad total volatility spillovers dominate the system and shift over time, implying that a pessimistic mood and uninformed traders, who tend to increase volatility and thus increase uncertainty (Avramov et al., 2006), dominate the financial markets.

Although Diebold and Yilmaz's (2009, 2012) spillover measures in combination with a VAR framework are extensively adopted in the current literature, a new framework based on the multivariate extension of the HAR model (VHAR) proposed by Corsi (2009) is on the rise to examine asymmetric volatility spillovers. The VHAR model is namely capable of capturing different stylized facts associated with volatility and its dynamics (Caloia et al., 2018), contrary to the widely used VAR models. Long memory, or the slow decline of the autocorrelation function, is one of the key characteristics of volatility series, and the VHAR model is able to capture this by considering many lags in a parsimonious way (Asai & Brugal, 2013). Furthermore, heterogeneity, or the fact that low-frequency volatility has a greater effect on subsequent high-frequency volatility than vice versa (Corsi, 2009), is a distinct feature of a volatility series that is captured by the VHAR specification since it models a 'cascade structure' of volatilities at various frequencies.

For example, Caloia et al. (2018) examine asymmetric volatility spillovers between five Economic and Monetary Union (EMU) countries their stock markets using a VHAR model in combination with the Diebold and Yilmaz (2012) methodology. They find that asymmetries in bad and good volatility are significant and time-varying between 2000 and 2016. Lastly, Souček and Todorova (2013) propose an orthogonalized VHAR model to examine volatility spillovers between three international stock markets and the crude oil market. They find significant volatility spillovers between the stock markets and oil futures that emerge mostly during and after the global financial crisis of 2007-2008. Moreover, they conclude that volatility spillovers are largely driven by short term shocks.

3 Data

This study analyses the (asymmetric) volatility spillover effects between the crude oil market and three international stock markets. In order to do so, I include the S&P 500 (SPX) from Standard and Poor's in New York for the United States, the Euro Stoxx 50 (STO50) from Stoxx Limited in Zurich for Europe and the Nikkei 225 (N225) from Nihon Keizai Shimbum Inc. for Japan. The West Texas Intermediate (WTI) futures traded on the New York Mercantile Exchange is used for the crude oil market since it provides a benchmark for crude oil that serves as a reference price for both buyers and sellers (Wang & Wu, 2018). The stock market indices are free-float capitalization weighted price indices and represent major and highly liquid financial markets in the U.S., Europe and Asia. The daily realized variance (RV), negative semivariance (RS^-) and positive semivariance (RS^+) series, based on high-frequency five-minute returns, are directly obtained from Wang and Wu (2018) and range from January 2002 to December 2014 resulting in a total of 2784 total observations.

Given that the distribution of the realized variance and semivariance is not Gaussian, I follow Andersen et al. (2003) and perform a log-transformation on the data in order to obtain approximately Gaussian measures. The transformation adopted is obtained by first taking the square root of the realized variance and then the logarithm. The same transformation is adopted to the positive and negative realized semivariance.

The descriptive statistics for the log transformation of the volatility measures are presented in Table 1. First of all, note that the average realized volatility of the crude oil market is higher compared to that of the three stock markets. This indicates that the crude oil market is much more volatile than the three stock markets and thus experiences more price fluctuations. Secondly, the similarity of the mean and standard deviation of the negative and positive semivariance could indicate that both types of volatility measures are very similar and asymmetries are not present. However, this similarity is misleading. Differences in volatility measures namely do not relate to their individual properties but to their correlations. Additionally, note that due to the log transformation almost all time series are approximately Gaussian with a skewness and kurtosis close to 0 and 3, respectively. Nonetheless, normality is still rejected by the Jarque-Bera test. Finally, the null hypothesis that a unit root is present in the time series is rejected for every volatility measure time series by the Augmented Dickey-Fuller test. Hence, all time series are stationary.

Table 1

Descriptive statistics for the realized volatility and realized semi-volatility

Series	Mean	St. dev.	Skewness	Kurtosis	JB	Min	Max	ADF
$log\sqrt{RV}$								
WTI	-3.503	0.552	0.257	2.706	40.633***	-4.703	-2.092	-4.366***
SPX	-4.997	0.523	0.649	3.284	204.972***	-6.030	-3.419	-4.843***
N225	-4.844	0.443	0.371	3.253	71.280***	-5.803	-3.481	-4.932***
STO50	-4.706	0.496	0.374	2.715	74.233***	-5.696	-3.416	-3.632***
$log\sqrt{RS^-}$								
WTI	-3.850	0.556	0.251	2.710	39.098***	-5.084	-2.444	-4.397***
SPX	-5.370	0.558	0.493	2.973	112.920***	-6.473	-3.780	-4.319***
N225	-5.238	0.495	0.282	2.989	36.989***	-6.361	-3.826	-5.320***
STO50	-5.070	0.531	0.309	2.669	57.152***	-6.177	-3.714	-3.422**
$log\sqrt{RS^+}$								
WTI	-3.871	0.564	0.257	2.699	41.072***	-5.061	-2.415	-4.492***
SPX	-5.357	0.524	0.712	3.424	256.331***	-6.347	-3.732	-4.644***
N225	-5.240	0.473	0.373	3.118	66.442***	-6.271	-3.840	-5.183***
STO50	-5.073	0.497	0.405	2.833	79.307***	-6.085	-3.729	-3.385**

Note. The total number of observations for each time series is 2784; JB shows the Jarque-Bera test statistic for normality; ADF shows the Augmented Dickey-Fuller test statistic for stationarity; ** $p < 0.05$, *** $p < 0.01$.

4 Methodology

In this section I introduce the concepts of realized variances and semivariances. After that, I describe the empirical methodology that is based on the VAR model used in Wang and Wu (2018) and the VHAR model used in Caloia et al. (2018), where I combine both models with the DAG technique advocated by Swanson and Granger (1997). Then, I describe the volatility spillover indices that are based on the variance decompositions from the aforementioned models. Finally, I explain how the models are evaluated.

4.1 Realized variance and semivariance

This paper analyses volatility asymmetries between the oil market and international stock markets. To model volatility, I use realized variances because they can be used as a proxy for the integrated variance (Andersen & Bollerslev, 1998). Then, for a specific trading day t, the daily realized variance estimator can be calculated as the sum of the squared intraday returns $r_{t,j}$:

$$RV_t = \sum_{j=1}^{M} r_{t,j}^2 \tag{1}$$

where M is the number of intraday (equally-spaced) observations and $j = 1/M$ is the given sampling interval. Note that the larger the number of intraday observations M, the closer the value of the realized variance lies to the true value of the integrated variance. Barndorff-Nielsen and Shephard (2002) namely show that the realized variance estimator converges to the integrated variance as $M \to \infty$.

To determine asymmetries in volatility spillovers, I follow Barndorff-Nielsen et al. (2008) and decompose the realized variance into negative and positive realized semivariances, RS^- and RS^+ respectively. The RS^- and RS^+ are defined as follows:

$$RS_t^- = \sum_{j=1}^{M} I(r_{t,j} < 0) r_{t,j}^2 \tag{2}$$

$$RS_t^+ = \sum_{j=1}^{M} I(r_{t,j} \geq 0) r_{t,j}^2 \tag{3}$$

where I is an indicator function. Barndorff-Nielsen et al. (2008) show that $RV_t = RS_t^- + RS_t^+$ and as a result, the realized semivariances can be used to measure downside (RS_t^-) and upside risk (RS_t^+). Then, according to Segal et al. (2015) a negative (positive) semivariance corresponds to a bad (good) state of the underlying variable and can thus serve as a proxy for bad (good) volatility.

4.2 VAR model

To model the volatility dynamics, I employ two models. The starting point for the first model is the (reduced-form) VAR model of Sims (1980). In a VAR model, each variable is explained by its own lagged values and the lagged values of the other variables in the system (Das, 2019). Hence, it is able to examine the dynamic relationships over time that exist between the variables. The (reduced-form) VAR(p) model with p lags for the realized variance is given by:

$$RV_t = \mu + \sum_{i=1}^{p} \Phi_i RV_{t-i} + \epsilon_t \tag{4}$$

where $RV_t = (RV_{1t}, ..., RV_{Nt})'$ is an N-dimensional vector holding the realized variance of N market indices, μ is an N-dimensional vector of constants, Φ is the $N \times N$ matrix of dynamic coefficients and ϵ_t is an N-dimensional vector of residuals which are assumed to be white noise and normally distributed. By definition, ϵ_t is white noise if $E(\epsilon_t) = 0$, $E(\epsilon_t \epsilon_t') = \Sigma_\epsilon$, and ϵ_t and ϵ_s are independent for $s \neq t$ with finite fourth moments (Franses et al., 2014).

The VAR model depends crucially on the choice of the lag order p since all results that follow after that are based on the chosen lag order (Hatemi-j, 2003). The optimal lag order can be determined by information criteria that often have one of the two following objectives; to make good forecasts or to pick the correct VAR order. In the former case, the lag order p should be chosen such that it minimizes some prediction criterion. In the latter case, the estimator of p should be consistent, i.e. $\lim_{T\to\infty} P(\widehat{p} = p) = 1$ (Wang, 2021). Since I want to determine the correct VAR order, I thus need to use information criteria that find a consistent estimator of p. Therefore, the Bayesian Information Criterion (BIC) by Schwarz (1978) and the Hannan-Quinn Criterion (HQ) by Hannan and Quinn (1979) are used, which are consistent for a stationary VAR process with standard white noise (Wang, 2021). The explicit formulas for the BIC and HQ are included in Appendix B.

Finally, after having selected the number of lags and concluded that the VAR model is stable, which is described in Section 4.7, the reduced-form parameters in Equation (4) are estimated using ordinary least squares (OLS).

4.3 VHAR model

In addition to the refined VAR model that was used by Wang and Wu (2018), I also implement a multivariate extension of the HAR (VHAR) model by Corsi (2009). As mentioned in the introduction, volatility spillovers based on the VHAR model are also considered as this model is able to capture the different stylized facts associated with volatility. Therefore, this might result in different asymmetric spillovers. Despite the fact that the VHAR model is not a long memory process, it is capable of reproducing the long-memory feature of volatility series by parsimoniously considering many lags (Asai & Brugal, 2013). One might then think that increasing the number of lags in the VAR also captures the long-memory behaviour of volatility. This is true, however by increasing the number of lags in the VAR, the dimensionality issue would be severe, especially with large sample sizes (Caloia et al., 2018).

The heterogeneous transmission of volatility is another important stylized fact captured by the VHAR model, as volatility over longer time intervals has a greater explanatory power on volatility over shorter time intervals than vice versa (Corsi, 2009). This feature is accounted for by assuming a hierarchical process in which partial volatilities are dependent on previous partial volatilities (Caloia et al., 2018). The VHAR for the realized variance can be written as follows:

$$RV_t^{(d)} = \mu + \phi^{(d)} RV_{t-1}^{(d)} + \phi^{(w)} RV_{t-1}^{(w)} + \phi^{(m)} RV_{t-1}^{(m)} + \varepsilon_t \tag{5}$$

where ε_t is an N-dimensional vector of residuals which are assumed to be white noise and normally distributed, $RV_t^{(d)} = \left(RV_{1t}^{(d)}, ..., RV_{Nt}^{(d)}\right)'$, $RV_t^{(w)} = \left(RV_{1t}^{(w)}, ..., RV_{Nt}^{(w)}\right)'$, $RV_t^{(m)} = \left(RV_{1t}^{(m)}, ..., RV_{Nt}^{(m)}\right)'$ are three $N \times 1$ vectors of daily, weekly and monthly realized variances and ϕ are $N \times N$ coefficient matrices. More specifically, $RV_t^{(w)} = \frac{1}{5}(\sum_{i=0}^{4} RV_{t-i})$ and $RV_t^{(w)} = \frac{1}{22}(\sum_{i=0}^{21} RV_{t-i})$. Note that the VHAR model in Equation (5) is essentially a VAR model with exogenous variables of lag order 1 (VARX(1)) where the exogenous variables are the weekly and monthly realized variances. Hence, similar to a regular VAR model, Equation (5) can be estimated via OLS. Moreover, the VHAR model can also be written as a constrained VAR(22) model. This can easily be seen by noting that the model in Equation (5) can be written as:

$$RV_t^{(d)} = \mu + \sum_{i=1}^{22} \beta_i^{(d)} RV_{t-i}^{(d)} + \epsilon_t \tag{6}$$

where the β coefficients are subject to the following constraints:

$$\beta_i = \begin{cases} \phi^{(d)} + \frac{1}{5}\phi^{(w)} + \frac{1}{22}\phi^{(m)} & \text{for} \quad i = 1 \\ \frac{1}{5}\phi^{(w)} + \frac{1}{22}\phi^{(m)} & \text{for} \quad i = 2, ..., 5 \\ \frac{1}{22}\phi^{(m)} & \text{for} \quad i = 6, ..., 22 \end{cases} \tag{7}$$

4.4 DAG technique

After having estimated the VAR model and VHAR model, the variance decompositions have to estimated. In order to do this, note that I can rewrite Equation (4) and Equation (6) as an infinite moving average process:

$$RV_t = \sum_{i=1}^{\infty} A_i \epsilon_t \tag{8}$$

where A_i is an $N \times N$ coefficient matrix, which is obtained from the recursion $A_i = \sum_{j=1}^{p} \Phi_j A_{i-j}$

where A_0 is the identity matrix $A_0 = I_n$ and $A_i = 0$ for $i < 0$. The moving average representation in Equation (8) is essential for understanding the system's dynamics, because it allows for variance decompositions to be computed (Wang & Wu, 2018). In fact, the error term from H-step-ahead forecast of the RV_t conditional on the information available at $t-1$ and its variance-covariance matrix are given by:

$$\xi_{t,H} = \sum_{h=0}^{H-1} A_h \epsilon_{t+H-h} \tag{9}$$

$$\mathrm{Cov}(\xi_{t,H}) = \sum_{h=0}^{H} A_h \Sigma_\epsilon A_h' \tag{10}$$

where Σ_ϵ is the variance-covariance matrix of the error term in Equation (4). Then, using forecast error variance decompositions, I can determine for each variable how much of its variance is explained by it's own shocks and how much of its variance is explained by shocks in the other variables. Previous research (e.g. Diebold and Yilmaz (2009)) mainly relied on the Cholesky decomposition for this, which assumes that the underlying shocks have a specific recursive contemporaneous causal structure. However, Yang and Zhou (2017) note that economic theories seldom offer guidance for the recursive causal structure and therefore the imposed restrictions are often arbitrary.

To solve this issue, I follow Yang and Zhou (2017) and Wang and Wu (2018) and make use of the DAG technique advocated by Swanson and Granger (1997) in order to identify the VAR structure. An advantage of the DAG technique is that it allows the data to speak for itself about the contemporaneous causality, resulting in a more credible ordering of the variables that identify the VAR structure (Swanson & Granger, 1997). Pan et al. (2019) describe the basic idea behind a DAG analysis as follows. A causal relationship between two variables is represented by arrows. So, the lack of a causal relationship between X and Y is exhibited by an edge missing between them. If the two variables have a correlation but no causal relationship, an edge without direction is displayed (X $-$ Y). In addition, the one-sided edge (X $\rightarrow$ Y) shows that the causal relationship is from X to Y and that X causes Y. Finally, the two-sided edge (X $\leftrightarrow$ Y) denotes the effect of X and Y on one another at the same time.

To obtain the DAGs, the PC algorithm introduced by Spirtes et al. (2001) is applied to the residuals of the models. In short, using Hoover (2005), the PC algorithm is performed as follows. Start with a complete directed graph and then first tests the unconditional correlation between each pair of variables. If no correlation is found, the edges are removed. Next, correlation between a pair of variables conditional on pairs, triples and so on is tested. Again, edges are removed if the conditional correlation is insignificant and as far as the data allows it. Finally, the algorithm determines the direction of the remaining edges. For the complete algorithm and a more elaborate explanation I refer to Spirtes et al. (2001) and Hoover (2005).

4.5 Volatility spillover indices

Following Wang and Wu (2018) I use volatility spillover indices that are similar to Diebold and Yilmaz (2014) their indices and that follow directly from the familiar notation of forecast error variance decomposition. The directional volatility spillover from market j to market i is defined as:

$$S^H_{i\leftarrow j} = \frac{\sum_{h=0}^{H-1} a^2_{h,ij}}{\sum_{h=0}^{H-1} \text{trace}(A_h A'_h)} \tag{11}$$

where $a_{h,ij}$ is the ijth element in the coefficient matrix of the moving average process A_h at step h, $\sum_{h=0}^{H-1} a^2_{h,ij}$ is the estimated contribution to the H-step-ahead error variance in forecasting volatility of market i due to shocks to volatility of market j and $\text{trace}(A_h A'_h)$ is the total H-step-ahead forecast error variation. Hence, the ratio in Equation (11) measures how much of the volatility spillovers in market i are due to shocks from market j.

Furthermore, the total directional spillover from other markets to market i and the total directional spillover to other markets from j are respectively defined as

$$S^H_{\bullet\to i} = \sum_{j=1,j\neq i}^{N} S^H_{i\leftarrow j} \tag{12}$$

$$S^H_{j\to\bullet} = \sum_{i=1,i\neq j}^{N} S^H_{i\leftarrow j} \tag{13}$$

Finally, the total volatility spillover index is defined as:

$$S^H = \frac{1}{N}\frac{\sum_{i,j=1;i\neq j}^{N} \sum_{h=0}^{H-1} a^2_{h,ij}}{\sum_{h=0}^{H-1} \text{trace}(A_h A'_h)} \tag{14}$$

The total spillover index measures the contribution of volatility shock spillovers to the total forecast error variance across individual markets (Wang & Wu, 2018).

According to Wang and Wu (2018), these volatility spillover indices complement the volatility measurements by Diebold and Yilmaz (2014) in two dimensions. First of all, the variance decompositions are extracted from the DAG-based structural VAR that is data-driven. Diebold and Yilmaz (2014), on the other hand, use Pesaran and Shin's (1998) ordering-free generated variance decompositions which still results in arbitrary imposed restrictions. Secondly, contrary to Diebold and Yilmaz (2014), the variance decompositions are estimated recursively for each period with an expanding sample, after the initial sample period. Estimating the spillovers recursively and with an expanding window, instead of a rolling window, can namely better capture volatility dynamics. This follows from Robinson (1995), whose long memory tests indicate that a shock's effect on early volatility is very persistent.

4.6 Asymmetric spillover indices

Asymmetric characteristics of the volatility can be examined by replacing the vector of realized variances $RV_t = (RV_{1t}, ..., RV_{Nt})'$ in Equations (4) and (6) with the vector of negative semivariances $RS_t^- = (RS_{1t}^-, ..., RS_{Nt}^-)'$ or the vector of positive semivariances $RS_t^+ = (RS_{1t}^+, ..., RS_{Nt}^+)'$. Then, similar to Baruník et al. (2016), Wang and Wu (2018) define the overall spillover asymmetry measure (SAM) as the difference between positive and negative spillovers:

$$SAM^H = S^{H+} - S^{H-} \tag{15}$$

where S^{H+} and S^{H-} are total volatility spillover indices due to positive semivariances (RS^+) and negative semivariances (RS^-), respectively, with an H-step-ahead forecast at time t. Hence, when SAM equals zero, spillovers arising from good and bad volatility are equal. Any deviation from zero gives rise to asymmetry in spillovers due to either good or bad volatility dominating.

Furthermore, to study the source of asymmetry among the markets, I follow Wang and Wu (2018) and decompose the SAM to obtain directional SAM spillovers. The spillover asymmetry measure received by market i from all other markets and transmitted by market i to all other markets are respectively given by:

$$SAM^H_{\bullet \to i} = S^{H+}_{\bullet \to i} - S^{H-}_{\bullet \to i} \tag{16}$$

$$SAM^H_{i \to \bullet} = S^{H+}_{i \to \bullet} - S^{H-}_{i \to \bullet} \tag{17}$$

These indices can then determine to what extent the volatility between market i and the other markets spillover asymmetrically. Moreover, it is worth emphasizing that these asymmetric volatility spillover indices complement the spillover measures of Baruník et al. (2016) in the same way as for the volatility spillover indices described at the end of Section 4.5.

4.7 Model diagnostics

Contrary to Wang and Wu (2018), I provide a more thorough evaluation on whether or not the VAR and VHAR models are correctly specified. The model is evaluated by checking the stationarity of the VAR and VHAR models and investigating the white noise properties and normality of the residuals. This provides valuable information about the model's fit and is crucial to endorse the quality of the results.

To check the stationarity of a VAR(p) model, note that first of all any VAR(p) process can be written in a first-order VAR form: the companion form. Secondly, any VAR(p) process that is stable is also stationary. Then, for a VAR(p) process to be stable, its reverse characteristic polynomial must have no roots in or on the complex unit circle (Wang, 2021). The reverse characteristic polynomial is defined as follows:

$$\det(I_K - A_1 z - ... - A_p z^p) = 0 \tag{18}$$

where I_K is the $K \times K$ identity matrix and A_i is the i^{th} coefficient matrix of the reduced form parameters. Moreover, checking if all roots are outside of the complex unit circle is equivalent to the condition that all eigenvalues of the companion matrix A have modulus less than 1 (Wang, 2021). Therefore, checking the stationarity of the models is done by retrieving the modulus of all eigenvalues of the companion matrix.

Next, I check the white noise properties of the residuals. The constant mean and variance property of the residuals can easily be checked by plotting the standardized residuals. To test the null hypothesis of no serial correlation left in the residuals, I employ the multivariate Portmanteau test by Hosking (1980). The test statistic is defined as:

$$Q_h = T^2 \sum_{i=1}^{h} \frac{1}{T-i} \mathrm{tr}(\hat{C}_i' \hat{C_0}^{-1} \hat{C}_i \hat{C_0}^{-1}) \sim \chi^2(K^2 h) \tag{19}$$

where h is the number of lags for which the autocorrelations are checked and where $\hat{C}_i = T^{-1} \sum_{t=i+1}^{T} \hat{u}_t \hat{u}_{t-i}'$ with $\hat{u}_t$ being the residuals.

Finally, the normality of the residuals is checked by the multivariate version of the Jarque-Bera (1987) test. The idea of this test is to compare the skewness and kurtosis of the standardized residuals with the skewness and kurtosis of the standard normal distribution. Hence, first I have to obtain the standardized residuals $\widehat{u}_t^s = (\widehat{u}_{1,t}^s, ..., \widehat{u}_{K,t}^s) = \widehat{\sum}_u^{-1/2} \widehat{u}_t$ where $\widehat{\sum}_u = T^{-1} \sum_t \widehat{u}_t \widehat{u}_t'$. Then, the multivariate Jarque-Bera test statistic is given by:

$$JB = Tb_1'b_1/6 + T(b_2 - 3_K)'(b_2 - 3_K)/24 \sim \chi^2(2K) \tag{20}$$

where $b_1 = (b_{11}, ..., b_{K1})'$ with $b_{k1} = T^{-1} \sum_t (\widehat{u}_{kt}^s)^3$, $b_2 = (b_{12}, ..., b_{K2})'$ with $b_{k2} = T^{-1} \sum_t (\widehat{u}_{kt}^s)^4$ and $3_K = (3, ..., 3)'$ is a $K \times 1$ vector.

5 Results

The results of this paper are obtained using the R (2021) software and its general statistical packages. Additionally, the packages 'pcalg' by Kalisch et al. (2012) and 'vars' by Pfaff et al. (2008) are used to obtain the DAGs and construct the VAR and VHAR models respectively. A short description of the code is provided in Appendix A.

5.1 DAG and SVAR results

The BIC and HQ criteria were used to determine the correct order for all VAR model specifications under consideration. Based on these criteria, which are shown in Table 8 in Appendix B, the lag length for all the VAR model specifications is set to $p = 5$. As mentioned before, the VHAR model specification is estimated by means of a VARX(1) where the exogenous variables are the weekly and monthly realized variances or realized semivariances.

The contemporaneous correlation matrices of the innovations from the VAR model in Equation (4) and the VHAR model in Equation (5) are given in Table 2. For the VAR model, strong correlations exist among the innovations of the STO50 and SPX and the STO50 and N225. Correlations between the stocks and oil markets on the other hand are small for both negative and positive semivariances. Moreover, the correlations for negative and positive semivariances show slightly distinct patterns. This could be due to asymmetry in the correlations of positive and negative semivariances between the stock and oil markets. Similar conclusions can be drawn for the VHAR model. Appendix C provides the correlation matrices between the positive and negative semivariances.

Table 2

VAR and VHAR residual correlation matrices

	VAR									VHAR								
	RS^-					RS^+					RS^-					RS^+		
	N225	STO50	WTI	SPX		N225	STO50	WTI	SPX		N225	STO50	WTI	SPX		N225	STO50	WTI	SPX
RS^-					RS^+					RS^-					RS^+				
N225	1.000	0.153	0.042	0.090	N225	1.000	0.045	0.004	0.064	N225	1.000	0.127	0.022	0.022	N225	1.000	0.079	-0.004	0.028
STO50	0.153	1.000	0.092	0.512	STO50	0.045	1.000	0.071	0.479	STO50	0.127	1.000	0.067	0.458	STO50	0.079	1.000	0.038	0.437
WTI	0.042	0.092	1.000	0.115	WTI	0.004	0.071	1.000	0.166	WTI	0.022	0.067	1.000	0.079	WTI	-0.004	0.038	1.000	0.128
SPX	0.090	0.512	0.115	1.000	SPX	0.064	0.479	0.166	1.000	SPX	0.022	0.458	0.079	1.000	SPX	0.028	0.437	0.128	1.000

Using the correlations between the residuals, the PC algorithm mentioned in Section 4.4 is applied in order to obtain the DAGs. The resulting directed graphs are shown in Figure 1 at a 10% significance level and display how volatility spreads from one market to another. Figures 1a and 1b show that according to the VAR model residuals the Japanese stock market (N225) is an exogenous source of positive as well as negative semivariances. It affects the negative semivariances in the European stock markets (STO50), while it affects the positive semivariances in the US stock market (SPX). Contrary to Wang and Wu (2018), the crude oil market (WTI) appears to be a receiver of negative semivariances. However, the oil market appears to be a transmitter of positive semivariances and based on the VHAR model, the crude oil market is an exogenous source of both positive and negative semivariances which is in accordance with Wang and Wu (2018). Similar to the VAR model, Figures 1c and 1d identify the Japanese stock market as a transmitter of positive as well as negative semivariances according to the VHAR model. Hence, both models find different contemporaneous causal flow patterns which in turn will influence the spillover indices.

Figure 1

Contemporaneous causal flow patterns based on the VAR and VHAR model

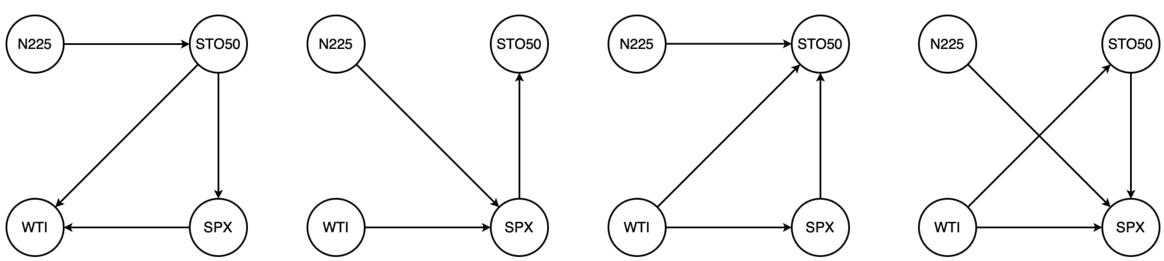

(a) RS^- *VAR* **(b)** RS^+ *VAR* **(c)** RS^- *VHAR* **(d)** RS^+ *VHAR*

Based on the contemporaneous causal flow patterns shown in Figure 1, zero restrictions are imposed on certain coefficients of the contemporaneous coefficient matrix of the SVAR representation. To ensure that these restrictions are valid and identify the model, LR tests for over-identification are performed. The results of these tests are shown in Table 3. Since all p-values of the test statistic are larger than the 10% significance level, the null hypothesis of valid restrictions cannot be rejected. Hence, the models are identified and the zero restrictions are valid.

Table 3

LR test for over-identification

Model	Chi-square statistic	Probability
Negative semivariances VAR	2.616	0.270
Positive semivariances VAR	1.092	0.779
Negative semivariances VHAR	2.455	0.293
Positive semivariances VHAR	0.716	0.699

Forecast error variance decompositions are computed based on the identified causal networks in Figure 1. Tables 4 and 5 present the forecast error variance decompositions for the VAR and VHAR at horizon H, which are due to prior shocks from other series as well as itself. The percentage describes the economic significance or magnitude of the causal relationships. Like Wang and Wu (2018), three different horizons, contemporaneous time ($H = 0$), short horizon ($H = 1$, 2) and long horizon ($H = 10$, 30), are used in order to evaluate how the effect of shocks change over time.

Table 4

Forecast error variance decomposition results VAR

Day	N225	STO50	WTI	SPX	Day	N225	STO50	WTI	SPX
Variance of N225 explained by shocks to realized negative semivariances					*Variance of N225 explained by shocks to realized positive semivariances*				
0	100.000	0.000	0.000	0.000	0	100.000	0.000	0.000	0.000
1	96.439	1.481	0.035	2.045	1	97.444	0.297	0.346	1.913
2	95.057	1.675	0.116	3.152	2	96.888	0.313	0.602	2.198
10	86.983	5.116	1.415	6.485	10	89.172	0.635	2.654	7.539
30	67.361	15.048	4.628	12.962	30	68.122	1.843	8.559	21.477
Variance of STO50 explained by shocks to realized negative semivariances					*Variance of STO50 explained by shocks to realized positive semivariances*				
0	2.329	97.671	0.000	0.000	0	0.092	77.067	0.629	22.213
1	2.886	94.527	0.054	2.532	1	0.461	69.738	2.375	27.426
2	3.264	93.317	0.119	3.300	2	0.744	66.128	2.521	30.608
10	7.570	86.604	0.583	5.243	10	2.608	53.877	4.331	39.185
30	15.853	72.023	2.540	9.584	30	8.374	37.026	8.177	46.422
Variance of WTI explained by shocks to realized negative semivariances					*Variance of WTI explained by shocks to realized positive semivariances*				
0	0.020	0.832	98.524	0.624	0	0.000	0.000	100.000	0.000
1	0.146	1.141	97.409	1.303	1	0.109	0.099	99.504	0.288
2	0.123	0.003	98.548	1.327	2	0.106	0.097	99.466	0.330
10	2.269	2.858	88.618	6.255	10	1.523	0.237	94.170	4.069
30	9.143	7.830	69.540	13.486	30	6.326	0.293	78.812	14.569
Variance of SPX explained by shocks to realized negative semivariances					*Variance of SPX explained by shocks to realized positive semivariances*				
0	0.611	25.608	0.000	73.782	0	0.400	0.000	2.742	96.858
1	1.507	26.531	0.168	71.794	1	0.657	0.025	4.548	94.770
2	2.166	26.909	0.217	70.709	2	0.812	0.023	4.851	94.314
10	6.210	31.632	2.580	59.579	10	3.492	0.936	10.047	85.524
30	15.701	34.850	6.094	43.355	30	10.339	2.953	15.012	71.696

Note. The forecast error variance decompositions are reported in percentage points. The variance decomposition is based on the DAGs in Figure 1.

The forecast error variance decompositions results for the VAR model are reported in Table 4. The variance decomposition of WTI for negative semivariances is rather substantial at day zero (98.524%) but as the horizon increases, a larger part of the variation is explained by shocks in the stock markets. This is in line with the earlier finding in Figure 1 that the WTI appears to be a receiver of negative semivariances. However, the WTI has a weak but growing impact on the three stock markets over all time horizons. Furthermore, the three stock markets appear to interact with one another at all time horizons, with the relationship between SPX and STO50 in particular appearing to be nontrivial. At all horizons, the shock to STO50 accounts for roughly 25% to 35% of the variation in SPX, whereas the opposite is noticeably weaker.

The forecast error variance decomposition results among realized positive semivariances are shown on the right hand side of Table 4. At day zero, the variance decomposition of N225 and WTI are both 100% explained by themselves, implying that they are solely driven by their own shocks (Wang & Wu, 2018). This result corresponds with the findings in Figure 1 that depict that the N225 and WTI are primarily exogenous sources of positive semivariances. Furthermore, both the STO50 and SPX have a large part of their variation explain by their own shocks at day zero. At all horizons, about 1% to 22% of N225 variation can be explained by the shock to SPX. This is noticeably larger than the combined effect of STO50 and WTI. More remarkable evidence is the result that the WTI shock explains a large percentage of the variation in the SPX, and that this is also true in the opposite case.

Table 5

Forecast error variance decomposition results VHAR

Day	N225	STO50	WTI	SPX	Day	N225	STO50	WTI	SPX
Variance of N225 explained by shocks to realized negative semivariances					*Variance of N225 explained by shocks to realized positive semivariances*				
0	100.000	0.000	0.000	0.000	0	100.000	0.000	0.000	0.000
1	98.940	0.178	0.036	0.847	1	98.862	0.462	0.121	0.555
2	98.762	0.229	0.041	0.967	2	98.683	0.568	0.124	0.625
10	98.744	0.237	0.042	0.976	10	98.666	0.580	0.124	0.629
30	98.744	0.237	0.042	0.976	30	98.666	0.580	0.124	0.629
Variance of STO50 explained by shocks to realized negative semivariances					*Variance of STO50 explained by shocks to realized positive semivariances*				
0	1.353	77.769	0.414	20.464	0	0.000	99.855	0.145	0.000
1	1.431	78.549	0.398	19.622	1	0.002	98.164	0.983	0.851
2	1.433	78.547	0.399	19.621	2	0.002	97.879	1.124	0.996
10	1.433	78.543	0.399	19.625	10	0.002	97.856	1.134	1.008
30	1.433	78.543	0.399	19.625	30	0.002	97.856	1.134	1.008
Variance of WTI explained by shocks to realized negative semivariances					*Variance of WTI explained by shocks to realized positive semivariances*				
0	0.000	0.000	100.000	0.000	0	0.000	0.000	100.000	0.000
1	0.013	0.015	99.879	0.093	1	0.000	0.304	99.672	0.024
2	0.018	0.018	99.855	0.109	2	0.000	0.357	99.603	0.040
10	0.019	0.018	99.852	0.111	10	0.000	0.362	99.594	0.045
30	0.019	0.018	99.852	0.111	30	0.000	0.362	99.594	0.045
Variance of SPX explained by shocks to realized negative semivariances					*Variance of SPX explained by shocks to realized positive semivariances*				
0	0.000	0.000	0.630	99.370	0	0.046	18.676	1.635	79.644
1	0.143	0.114	0.621	99.121	1	0.112	19.372	1.842	78.674
2	0.168	0.128	0.621	99.083	2	0.122	19.389	1.957	78.533
10	0.171	0.129	0.621	99.080	10	0.122	19.386	1.974	78.517
30	0.171	0.129	0.621	99.080	30	0.122	19.386	1.974	78.517

Note. The forecast error variance decompositions are reported in percentage points. The variance decomposition is based on the DAGs in Figure 1.

Table 5 presents the forecast error variance decompositions results for the VHAR model, which is able to capture the heterogeneity and long-memory of volatility. The first noticeable difference compared to the VAR model is the fact that for all series and at all time horizons, the variation of the series are largely explained by their own shocks. Two exceptions are the shock of SPX to the STO50 among negative semivariances and the shock of STO50 to SPX among positive semivariances. At day zero, the variance decomposition of N255 and WTI for negative semivariances are 100%, which again is in line with the earlier finding in Figure 1 that the N225 and WTI appear to exogenous sources of negative volatility. Furthermore, it is worth pointing out that as the horizon increases, a larger part of the variation in one series among negative semivariances is explained by shocks in other series albeit very small.

The forecast error variance decomposition results among the positive semivariances on the right hand side of Table 5 show similar results to the negative semivariances case. Variation of series are largely explained by their own shocks at all horizons, where at day zero 100% of the variation of N225 and WTI is explained by their own shocks. This is, again, consistent with the findings in Figure 1. Moreover, significant causal linkage appear to be existing between the STO50 and SPX. More specifically, about 18% to 20% of the SPX variation is explained by shocks to the STO50.

Based on these findings, it can thus be concluded that the VAR and VHAR models result in different causal linkages between the oil and stock markets. As a result, it can concluded that based on the VAR results, the markets are more connected. This follows from the fact that as the horizon increases, a larger fraction of a market's volatility is explained by the other markets. The VHAR results on the other hand indicate that only the STO50 and SPX are highly connected. Previous research indicates that financial markets and commodity markets have become more connected over the years (Broadstock et al., 2012; Zhang, 2017), especially after the global financial crisis. Therefore, the VAR results seem to be more consistent and in accordance with previous research.

5.2 Asymmetric results from DAG-based SVAR

The focus of this paper is the extent to which volatility spillovers are asymmetrical because of RS^{-} and RS^{+} and how they differ when using two different models. To this end, a comparison of forecast error variance decompositions between the negative and positive semivariances presented in Tables 4 and 5 is helpful. According to the results, WTI can explain a much higher percentage of variation in the other three markets in positive semivariance spillovers than in negative semivariance spillovers. This shows the dominance of good oil market uncertainties on global stock markets. Asymmetry in volatility spillovers refers to the differences between good and bad volatility spillovers. The differences between negative and positive semivariances in Tables 4 and 5 are noteworthy because they give additional empirical evidence of asymmetries in volatility spillovers between the oil and global stock markets (Wang & Wu, 2018). So, how can I compare the forecast error variance decompositions of both models?

The answer is network centrality and two measures that allow for such a comparison are provided by Ahern and Harford (2014). The results of these measures are shown in Table 6. In the network's adjacency matrix, degree centrality (DC) is defined as the average of the column sum of the off-diagonal total pairwise spillover intensities. Simply put, if a market's overall spillover intensity from and to others is higher, it is more central (Ahern & Harford, 2014). The principal eigenvector of the network's adjacency matrix is used to measure eigenvector centrality (EC). Intuitively, if a market is connected to other central markets, it is considered more central (Ahern & Harford, 2014).

Table 6

Network centrality

VAR										VHAR									
	RS^-					RS^+					RS^-					RS^+			
	N225	STO50	WTI	SPX		N225	STO50	WTI	SPX		N225	STO50	WTI	SPX		N225	STO50	WTI	SPX
RS^-					RS^+					RS^-					RS^+				
N225	0.000	12.686	3.684	12.695	N225	0.000	3.243	4.177	11.031	N225	0.000	1.670	0.044	1.147	N225	0.000	0.557	0.124	0.751
STO50	12.686	0.000	3.441	36.875	STO50	3.243	0.000	4.568	40.121	STO50	1.670	0.000	0.418	19.750	STO50	0.557	0.000	0.582	20.394
WTI	3.684	3.441	0.000	8.835	WTI	4.177	4.568	0.000	14.116	WTI	0.044	0.418	0.000	0.732	WTI	0.124	0.582	0.000	2.015
SPX	12.695	36.875	8.835	0.000	SPX	11.031	40.121	14.116	0.000	SPX	1.147	19.750	0.732	0.000	SPX	0.751	20.394	2.015	0.000
DC	9.688	17.667	5.320	19.468	DC	6.150	15.977	7.620	21.756	DC	0.954	7.279	0.398	7.210	DC	0.477	7.178	0.907	7.720
EC	0.369	0.635	0.201	0.648	EC	0.231	0.630	0.288	0.683	EC	0.099	0.704	0.041	0.703	EC	0.045	0.702	0.089	0.705

Note. The upper 4 × 4 submatrices are adjacency matrices in which the diagonal elements are zeros and the off-diagonal elements are 10-day-ahead total pairwise volatility spillover intensity (in percentage points). For example, the total negative volatility spillover intensity for the VAR model between N225 and STO50 is 12.686%, which is the sum of the N225 spillover to STO50, 7.570%, and the N225 spillover to N225, 5.116%.

For the VAR, both centrality measures are the highest for the SPX, showing that the US stock market is at the core of the oil and global stock market volatility spillover network. Most importantly, Table 6 allows for distinguishing between good and bad volatility spillovers in terms of centrality. The N225 is more central than the WTI in good volatility spillovers, but in bad volatility spillovers, the opposite is true. Given this evidence, I can expect the oil market to be a greater source of uncertainty in positive returns in the network than the stock market in Japan.

The network centrality of the VHAR model is slightly different compared to that of the VAR. Both centrality measures are the highest for the SPX in bad volatility spillovers indicating that the US stock market is at the core of the oil and global stock market bad volatility spillover network. For the good volatility spillovers however, both centrality measures are the highest for the STO50, showing that it is at the heart of the good volatility spillover network. The same pattern regarding centrality of N225 and WTI as in the VAR case can be found for the VHAR case. Thus, also here N225 is more central in good volatility spillovers, while the WTI is more central in bad volatility spillovers. However, it is worth pointing out that the differences (asymmetry) in centrality measures attributable to good and bad volatility spillovers are small for both models.

5.3 Volatility spillover indices

Following Wang and Wu (2018), volatility spillover indices are constructed by estimating variance decompositions recursively each day with an expanding sample. The models are initialized with the first 200 observations. The 10-step-ahead forecast error variance decomposition matrix can then be obtained after each recursive estimation using Equation (11).

5.3.1 Total volatility spillover indices results

Before looking into asymmetries, I examine how connected the oil and global stock markets are. The total spillovers and volatility of individual markets are depicted in Figure 2. One might expect that rises (or declines) in the volatility of individual markets are matched by rises (or declines) in total volatility spillovers. Indeed, the individual market's volatility does play a key role in volatility spillover analysis. Generally, volatility spillovers increase in response to unexpected increases in the volatility levels of individual markets as can be seen in Figure 2. However, the sudden increase in total spillover around 2006 before the global financial crisis is quite remarkable. This applies for both the VAR and VHAR model and could be explained by the following event. Around this time, the US housing bubble burst, which eventually became the impetus for the subprime mortgage crisis in 2007-2008 (Baker, 2008; Levitin & Wachter, 2011) and could therefore have caused the sudden increase in volatility in the markets.

Figure 2

Total volatility spillover index and realized volatilities plots for the VAR and VHAR

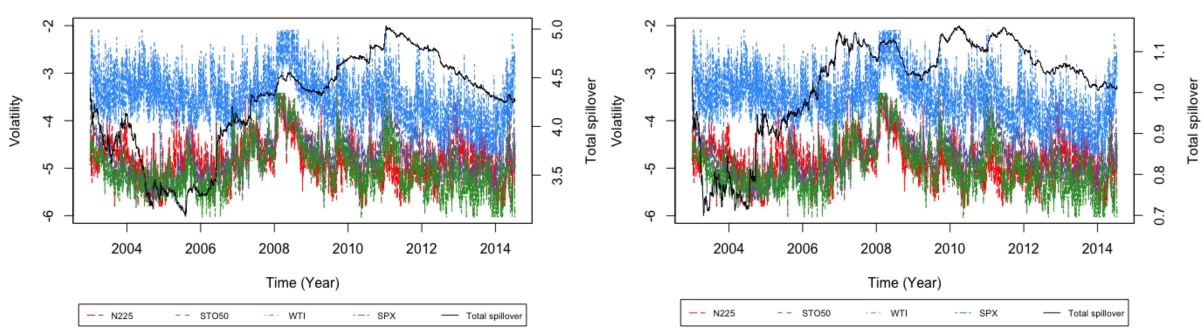

(a) *VAR* **(b)** *VHAR*

Regarding the global financial crisis, the total volatility spillover index based on the VAR model does indicate sudden increases of volatility in 2007 and 2008. The total volatility spillover index based on the VHAR model shows different results. Noticeable is the sharp increase of the index around 2005. Since the global financial crisis did not happen at that time it seems that the total volatility spillover index based on the VHAR model overreacts to an increase of the N225 around 2005. However, leading up to and during the global financial crisis, the index does increase sharply. Also, when comparing the indices based on the underlying model, the index based on the VHAR model tends to increase more gradually than the one based on the VAR. This result verifies the fact that the VHAR is better able at capturing the long-memory and heterogeneity of volatility.

A possible explanation for the increase in volatility around the global financial crisis is that it impacted all financial markets and changed how market participants perceive risk (Burns et al., 2012). As a result of more homogeneous perceptions among market participants, who now expect higher levels of risk measured by volatility, market connectedness increases post-crisis (Baruník et al., 2016). This follows from the higher levels of total volatility spillover indices post-crisis. Hence, based on Baruník et al. (2016) their reasoning, it can be concluded that the volatility spillovers are much higher due to homogeneous beliefs about growing risk as a result of the global financial crisis. For investors who have exposure to the oil market and stock markets such as portfolio managers, this finding can be useful as the strong linkages between oil and stock markets can limit the diversification benefits substantially (Xu et al., 2019). Moreover, the oil market has, on average, a higher volatility than stock markets, implying that market participants take on more risk on the oil market, receive higher returns on the oil market accordingly and are better able at predicting stock volatility than oil volatility (Wang & Wu, 2018).

5.3.2 Asymmetric volatility spillover indices

The main focus of this paper is asymmetric volatility spillovers. The results for the asymmetry in spillovers are given in Figure 3. Figures 3a and 3b show the total volatility spillovers as they change over time. Volatility spillovers from bad and good volatility are depicted in Figures 3c and 3d by two different lines. If these two lines align, the spillovers are symmetric and equivalent to the total volatility spillovers in Figures 3a and 3b. Any deviation from this equivalence motivates asymmetry (SAM) in volatility spillovers (Baruník et al., 2016). This is demonstrated in Figures 3e and 3f, which depicts the difference between the good and bad volatility spillovers.

Figure 3

Spillover measures and spillover asymmetry measures SAM

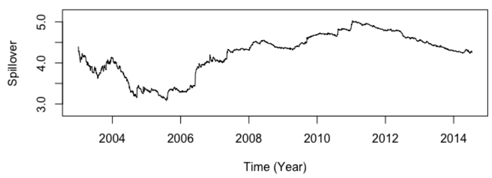

(a) *Total volatility spillover VAR*

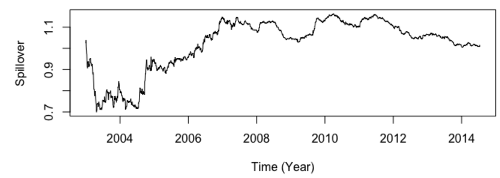

(b) *Total volatility spillover VHAR*

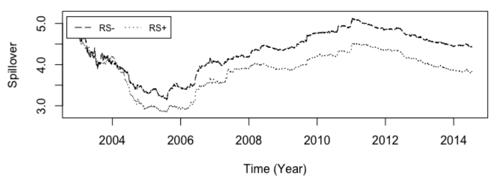

(c) *Total semivariances spillover VAR*

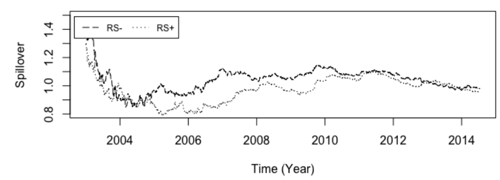

(d) *Total semivariances spillover VHAR*

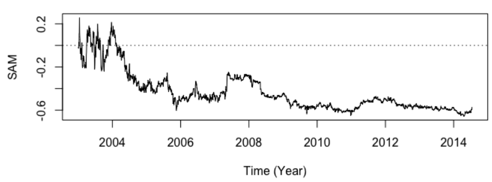

(e) *Spillover asymmetry measure VAR*

(f) *Spillover asymmetry measure VHAR*

Figures 3a and 3b show that the total volatility spillover is high during and after the global financial crisis for both models. However, in the period leading up to the global financial crisis, total volatility spillover is low. More importantly, from Figures 3c and 3d it can be concluded that volatility spillovers caused by bad and good volatility evolve in different ways, with bad volatility spillovers dominating good volatility spillovers. According to Avramov et al. (2006), positive returns are followed by sell activities that are dominated by informed traders who tend to reduce total volatility. Negative returns, on the other hand, are followed by sell activities that are dominated by uninformed traders who tend to increase total volatility. Hence, the negative $SAMs$ in Figures 3e and 3f imply that the whole system is dominated by uninformed traders.

The dynamic of the SAM reveals whether negative or positive spillovers are dominant and according to Wang and Wu (2018), it can therefore be used as a proxy for negative and positive market expectations. They describe that the SAM assesses how sensitive the majority of market participants are to bad or good news, as well as how the news spreads across markets. Thus, the SAM can be used to determine if the markets are in a pessimistic or optimistic mood, as well as what the expectations are. Therefore, the presence of negative spillovers shows that a pessimistic mood prevailed throughout most of the sample period. However, the path of the SAM depicted by the VAR is clearly different than the one depicted by the VHAR.

The results in Figure 3e namely show that, based on the VAR model, the overall mood on the market became more pessimistic after the global financial crisis. However, according to the VHAR results depicted in Figure 3f, the overall mood on the market first becomes more pessimistic after the global financial crisis before starting to become optimistic around 2014. So, which path seems more realistic? Previous research has shown that around 2014 bad volatility dominates good volatility resulting in a negative SAM (Wang & Wu, 2018; Xu et al., 2019). Hence, this indicates that a pessimistic mood would dominate the market around 2014, which is in accordance with the SAM based on the VAR model. The pessimistic mood could be explained by the announcement of the Organization of Petroleum Exporting Countries (OPEC) to not further reduce the oil supply and the Chinese economy slowing down (Xu et al., 2019). However, arguments can also be made for the path depicted by the VHAR model, albeit of less power since one would expect the SAM to be of a larger negative magnitude after the global financial crisis than before. The increasing SAM after the global financial crisis could be explained by the fact that market participants adjust their expectations, expect economic growth again and therefore become more optimistic. Nonetheless, based on the previous literature, a fast recovery of an optimistic mood on the market seems unrealistic and therefore the SAM based on the VAR model seems to display the market sentiment the best.

Finally, these results are also of interest to portfolio managers as the SAM can help determine whether a portfolio is well balanced or not (Baruník et al., 2016). In this case, I have an equally weighted portfolio consisting of the N225, STO50, WTI and SPX. On the total portfolio level, Figures 3e and 3f show that the SAM is negative for almost the whole sample period for both models. This indicates that the portfolio is not well balanced in the sense that the effects of bad volatility are larger than those of good volatility (Baruník et al., 2016). Moreover, it indicates that at the aggregate portfolio level asymmetry is present. Hence, to establish a more well balanced portfolio, further diversification or rebalancing of the portfolio weights is necessary.

5.3.3 Contribution of individual markets to asymmetry

To round up the analysis, I examine the individual market's contribution to asymmetry which uncovers additional information regarding asymmetries. The individual markets' directional spillover asymmetry measures $SAM^H_{i\to\bullet}$ and $SAM^H_{\bullet\to i}$ are shown in Figures 4 and 5 for both models.

Figure 4

Directional spillover asymmetry measure $SAM^{H}_{i\to\bullet}$ *and* $SAM^{H}_{\bullet\to i}$ *for the VAR model*

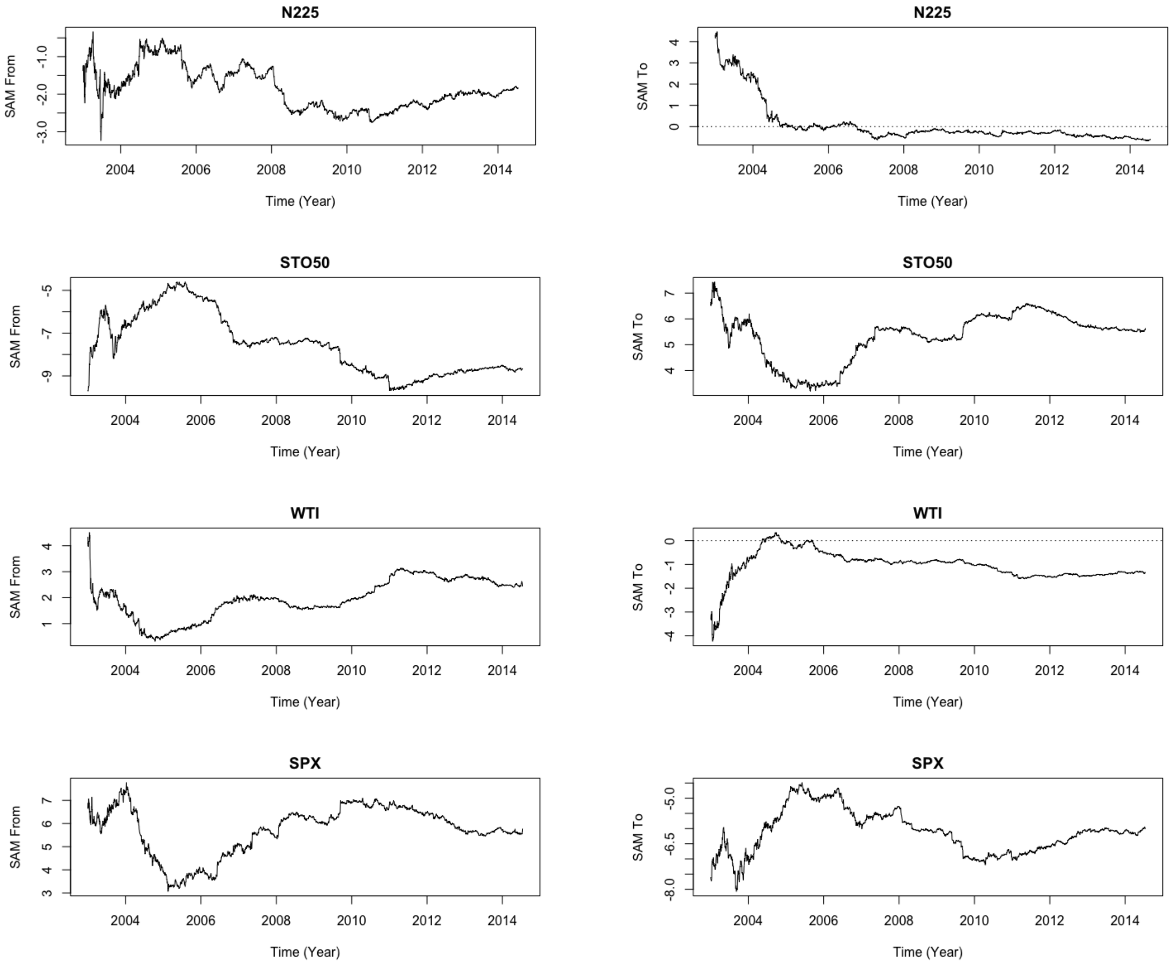

Figure 4 depicts the SAM results based on the VAR model. In 2006 and 2007, the WTI showed positive spillovers to other markets and stable spillovers from other markets, reflecting the higher price of oil as a result of rising conflicts between Israel and Lebanon and the ongoing Iraq war, where the Iraqi government tried to reclaim control of national security (Spirling, 2007). Stock markets experienced huge price drops and fluctuations during the global financial crisis, and because they interacted with one another, this resulted primarily in lower or negative spillovers. The oil market, on the other hand, continued to perform well throughout the global financial crisis, which could be attributed to continuing high demand from China and emerging markets (Wang & Wu, 2018). Moreover, it is worth noting that the SPX transmitted positive spillovers to other markets during the global financial crisis while the STO50 received positive spillovers from the other markets. This is in correspondence with the causal flow patterns found in Figure 1b and therefore not surprising.

Figure 5

Directional spillover asymmetry measure $SAM^H_{i\to\bullet}$ and $SAM^H_{\bullet\to i}$ for the VHAR model

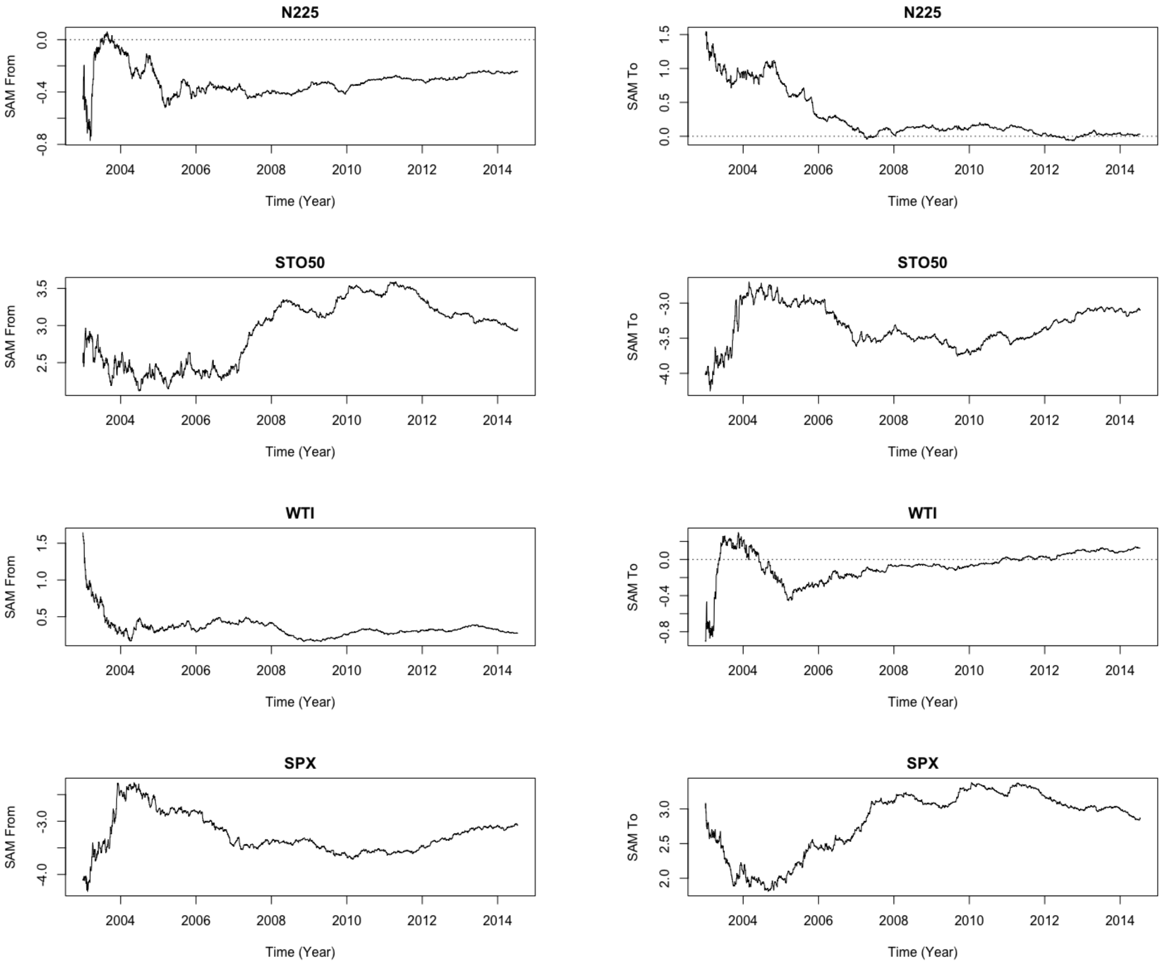

The directional SAM results based on the VHAR model are given in Figure 5. Similar spillover results are found for the N225. Moreover, also here the WTI shows positive spillovers to other markets and increasing spillovers from other markets throughout the global financial crisis. Compared to the $SAMs$ constructed by the VAR, the SPX now receives positive spillovers during the global financial crisis instead of transmitting them to other markets. Moreover, the STO50 now transmits positive spillovers to the other markets instead of receiving them. Based on the causal flow patterns in Figure 1d, this is not surprising. However, explaining this difference compared to the VAR model is ambiguous as the causal flow patterns are based on the residuals of the models. One possible explanation could be the fact that the realized semivariances do exhibit long-memory and heterogeneity, which is only captured by the VHAR model.

To date, a lot of research has been done on uncertainty in the oil market and has shown that uncertainty in the oil market has a detrimental impact on the global economy, which jeopardizes the recovery of global stock markets (Masih et al., 2011; Wang et al., 2013). The prominent negative spillovers in Figures 4 and 5 reflect the pessimistic market sentiment during the sample period that was already discovered in Section 5.3.2. Meanwhile, during and after the global financial crisis, the oil market has mostly seen positive or increasing spillovers from other markets according to both models. An explanation for this could be that since the commencement of the global financial crisis and the global economic recovery, the global economy has become increasingly reliant on oil (Wang & Wu, 2018). As a result of the increased oil demand, oil prices rise which in turn increases the positive spillovers received from the stock markets. From an investor's perspective, this finding indicates that the oil market can be considered as a safe haven or hedge against financial crises. Including oil futures in a portfolio can therefore offset the decline in returns in the stock markets.

5.4 Model diagnostics and robustness check

To asses whether or not the models are correctly specified, stationarity and the white noise properties as well as the normality of the residuals are checked. Moreover, a robustness check is performed. The modulus of all eigenvalues of the companion matrix are displayed in Figure 6. For both models and both series, all modulus of the eigenvalues are within the unit circle. This indicates that the models are stable and thus covariance stationary.

Figure 6

Results stability test

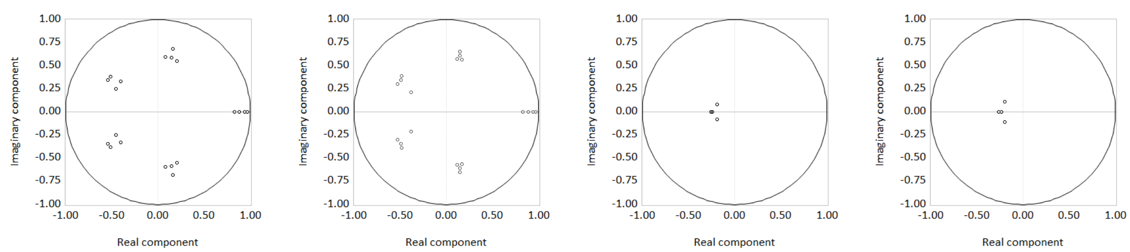

(a) RS^- *VAR* **(b)** RS^+ *VAR* **(c)** RS^- *VHAR* **(d)** RS^+ *VHAR*

Table 7 presents the results from the multivariate Portmanteau test for autocorrelation up to lag 10 and the multivariate Jarque-Bera test for normality. Based on these results, it can be concluded that for negative as well as positive semivariances and for both model specifications the null hypotheses are rejected. Hence, significant autocorrelations are still present in both the residuals of the VAR and VHAR models and the residuals are also not jointly normally distributed.

To check the white noise properties of a constant mean and variance plots of the standardized residuals are provided in Appendix D. From these plots it can easily be derived that the residuals approximately follow a white noise process for both models and semivariances.

Table 7

Residual correlation and normality test results

	VAR		VHAR	
Test statistic	RS^-	RS^+	RS^-	RS^+
Q_{10}	252.545***	242.944***	1479.030***	1422.438***
JB	379.363***	461.010***	224.811***	257.048***

Note. Q_{10} shows the multivariate Portmanteau test statistic for residual autocorrelation up to lag 10; JB shows the multivariate Jarque-Bera test statistic for normality; *** $p < 0.01$.

Based on these findings, it can thus be concluded that models are stationary, however not correctly specified because of the significant autocorrelations and non-normality of the residuals. Therefore, the models fail to capture the data generating process accurately. The results may therefore be flawed due to the poor specification of the models.

Figure 7

Robustness check spillover measures.

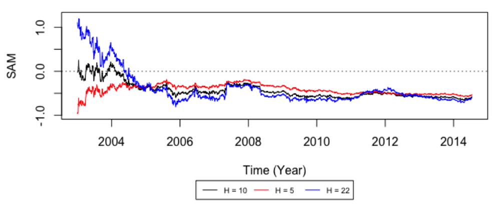

(a) *Spillover asymmetry measure VAR*

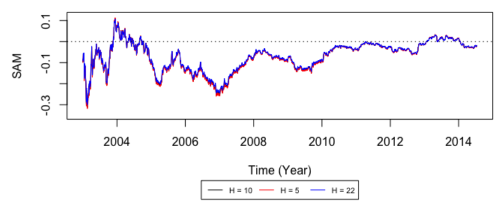

(b) *Spillover asymmetry measure VHAR*

Finally, to check the robustness of the results, I implement two different variance decomposition forecast horizons, namely one-week-ahead ($H = 5$) and one-month-ahead ($H = 22$). The results of the robustness checks for the spillover asymmetry measures are presented in Figure 7. The robustness check for the total volatility spillover and total semivariances spillover are provided in Figure 12 in Appendix D. It becomes apparent that the number of observations used to initialize the VAR model heavily influences the spillover asymmetry measures in the first year after the initialization. However, after that the results do not seem to differ depending on their forecast horizon. Hence, the results from the VAR model can be considered robust. The initialization does not seem to influence the VHAR model. Given the structure of the VHAR model, this is not surprising. Hence, it can be concluded that the results from the VHAR model are robust as well.

6 Conclusion

This paper aims at shedding a new light on asymmetries in volatility spillovers by examining whether taking into account the different stylized facts associated with volatility leads to better insights between the crude oil and three global stock markets. The analysis is performed by utilizing the DAG technique and good and bad volatility in a refined structural VAR and VHAR framework. In addition to the traditional VAR framework, the VHAR specification is used as it is able to capture the long-memory and heterogeneity of volatility. Then, based on the DAG and structural VAR and VHAR results, I examine the static and dynamic characteristics of asymmetric volatility spillovers.

Firstly, according to the DAG results based on the VAR model the Japanese market is an exogenous source of good and bad volatility in the contemporaneous time. The oil market was found to be a receiver of negative spillovers, contrary to previous research (Wang & Wu, 2018). The DAGs based on the VHAR model on the other hand, did indicate that the oil market is an exogenous source of negative and positive volatility spillovers. This could imply that the oil market does display the long-memory and heterogeneity characteristics that are captured by the VHAR.

Secondly, asymmetries in volatility spillovers are present throughout the system. The forecast error variance decomposition for example showed that for both models, the oil market is able to explain a substantially higher percentage of variation in international stock markets in positive volatility spillovers than it can in negative volatility spillovers. However, it was found that for the VHAR model shocks to the realized negative and positive semivariances of the financial markets are largely explained by themselves which is contrary to previous research. Furthermore, due to the presence of positive and negative volatility spillovers, asymmetries in network centrality were also found. Both models found the European market and U.S. market to be the most central.

Thirdly, the spillover indices showed that asymmetries in volatility spillovers change over time. Both models showed that bad volatility spillovers dominate good volatility spillovers over the sample period. However, the VAR model showed that after the global financial crisis bad volatility spillovers became more prominent than good volatility spillovers. This implies that the overall market sentiment became more and more pessimistic. The VHAR model on the other hand, showed that a few years after the global financial crisis good volatility spillovers started dominating the market indicating that the market became more optimistic. A striking difference between the two models, which could be explained by the different causal linkages found by the DAGs. The negative spillover asymmetry measure over the sample period for both models also indicates that a portfolio consisting of the N225, STO50, WTI and SPX is not well balanced and that more diversification benefits can be attained. Furthermore, during and after the global financial crisis prominent positive spillovers from the oil market to the other markets were found. From an investor's perspective, this indicates that oil futures can be considered as a hedge against financial crises. Including oil futures in a portfolio can therefore offset the price drops in the stock markets.

To summarize, I find that overall bad volatility spillovers tend to dominate good volatility spillovers. This finding has important implications for investors as this implies that negative volatility spillovers appear to be the most common risk spillovers in the network. Moreover, including the VHAR model in the analysis to account for the different stylized facts associated with volatility does not provide better insights in the asymmetric volatility spillovers. This conclusion is based on the fact that the VHAR model results are inconsistent with previous research.

7 Discussion

This paper has several limitations. First of all, contrary to Wang and Wu (2018), no restrictions are imposed to address the non-synchronous trading problem. Hence, the Japanese market could still influence the U.S. market in the contemporaneous time even though the Japanese market is closed when the U.S. market is open. This resulted in different DAG results compared to those found by Wang and Wu (2018). Nonetheless, their DAGs show that show a contemporaneous causal link between Japan and the U.S. as well. As a result, the spillovers are also different compared to Wang and Wu (2018) since they are determined by the DAG results. Hence, I was unable to replicate the results of their paper exactly. Second, the PC algorithm shows very different DAGs based on the significance level chosen. Therefore, the validity of the contemporaneous causal flow patterns is questionable. Third, the residuals of both models do not satisfy all white noise properties and are not normally distributed. To improve further results, structural breaks, a higher lag order or error distribution with fatter tails such as the Student's t-distribution should be considered.

For future research it might be interesting to look at the COVID-19 pandemic and see how that crisis influences volatility spillovers between the oil market and stock markets. Different result are expected as due to the pandemic a lot of (international) traffic was slowed down or put on hold, resulting in the economy being less reliant on oil than during the global financial crisis. Oil futures might therefore not have been able to hedge against stock market declines during the COVID-19 pandemic as they did during the global financial crisis.

References

Acemoglu, D., & Zilibotti, F. (1997). Was prometheus unbound by chance? Risk, diversification, and growth. *Journal of Political Economy*, *105*(4), 709–751.

Ahern, K. R., & Harford, J. (2014). The importance of industry links in merger waves. *The Journal of Finance*, *69*(2), 527–576.

Andersen, T. G., & Bollerslev, T. (1998). Answering the skeptics: Yes, standard volatility models do provide accurate forecasts. *International Economic Review*, 885–905.

Andersen, T. G., Bollerslev, T., Diebold, F. X., & Labys, P. (2003). Modeling and forecasting realized volatility. *Econometrica*, *71*(2), 579–625.

Arouri, M. E. H., Jouini, J., & Nguyen, D. K. (2011). Volatility spillovers between oil prices and stock sector returns: Implications for portfolio management. *Journal of International Money and Finance*, *30*(7), 1387–1405.

Asai, M., & Brugal, I. (2013). Forecasting volatility via stock return, range, trading volume and spillover effects: The case of Brazil. *The North American Journal of Economics and Finance*, *25*, 202–213.

Avramov, D., Chordia, T., & Goyal, A. (2006). The impact of trades on daily volatility. *The Review of Financial Studies*, *19*(4), 1241–1277.

Baker, D. (2008). The housing bubble and the financial crisis. *Real-world Economics Review*, *46*(20), 73–81.

Barndorff-Nielsen, O. E., Kinnebrock, S., & Shephard, N. (2008). Measuring downside risk, realised semivariance. *CREATES Research Paper*, (2008-42).

Barndorff-Nielsen, O. E., & Shephard, N. (2002). Estimating quadratic variation using realized variance. *Journal of Applied Econometrics*, *17*(5), 457–477.

Bartram, S. M., Brown, G., & Stulz, R. M. (2012). Why are US stocks more volatile? *The Journal of Finance*, *67*(4), 1329–1370.

Baruník, J., Kočenda, E., & Vácha, L. (2016). Asymmetric connectedness on the US stock market: Bad and good volatility spillovers. *Journal of Financial Markets*, *27*, 55–78.

Bessler, D. A., & Yang, J. (2003). The structure of interdependence in international stock markets. *Journal of International Money and Finance*, *22*(2), 261–287.

Bouri, E. (2015). Oil volatility shocks and the stock markets of oil-importing MENA economies: A tale from the financial crisis. *Energy Economics*, *51*, 590–598.

Broadstock, D. C., Cao, H., & Zhang, D. (2012). Oil shocks and their impact on energy related stocks in China. *Energy Economics*, *34*(6), 1888–1895.

Burns, W. J., Peters, E., & Slovic, P. (2012). Risk perception and the economic crisis: A longitudinal study of the trajectory of perceived risk. *Risk Analysis: An International Journal*, *32*(4), 659–677.

Caloia, F. G., Cipollini, A., & Muzzioli, S. (2018). Asymmetric semi-volatility spillover effects in EMU stock markets. *International Review of Financial Analysis*, *57*, 221–230.

Chen, N.-F., Roll, R., & Ross, S. A. (1986). Economic forces and the stock market. *Journal of Business*, 383–403.

Corbet, S., Hou, Y. G., Hu, Y., Oxley, L., & Xu, D. (2021). Pandemic-related financial market volatility spillovers: Evidence from the Chinese COVID-19 epicentre. *International Review of Economics & Finance*, *71*, 55–81.

Corsi, F. (2009). A simple approximate long-memory model of realized volatility. *Journal of Financial Econometrics*, *7*(2), 174–196.

Das, P. (2019). Econometrics in Theory and Practice. *Springer*, *10*, 978–981.

Diebold, F. X., & Yilmaz, K. (2009). Measuring financial asset return and volatility spillovers, with application to global equity markets. *The Economic Journal*, *119*(534), 158–171.

Diebold, F. X., & Yilmaz, K. (2012). Better to give than to receive: Predictive directional measurement of volatility spillovers. *International Journal of Forecasting*, *28*(1), 57–66.

Diebold, F. X., & Yilmaz, K. (2014). On the network topology of variance decompositions: Measuring the connectedness of financial firms. *Journal of Econometrics*, *182*(1), 119–134.

Fengler, M. R., & Gisler, K. I. (2015). A variance spillover analysis without covariances: What do we miss? *Journal of International Money and Finance*, *51*, 174–195.

Filis, G., Degiannakis, S., & Floros, C. (2011). Dynamic correlation between stock market and oil prices: The case of oil-importing and oil-exporting countries. *International Review of Financial Analysis*, *20*(3), 152–164.

Franses, P. H., van Dijk, D., & Opschoor, A. (2014). *Time Series Models for Business and Economic Forecasting*. Cambridge University Press.

Guesmi, K., & Fattoum, S. (2014). Return and volatility transmission between oil prices and oil-exporting and oil-importing countries. *Economic Modelling*, *38*, 305–310.

Hamilton, J. D. (1983). Oil and the macroeconomy since World War II. *Journal of Political Economy*, *91*(2), 228–248.

Hammoudeh, S., Yuan, Y., Chiang, T., & Nandha, M. (2010). Symmetric and asymmetric US sector return volatilities in presence of oil, financial and economic risks. *Energy Policy*, *38*(8), 3922–3932.

Hannan, E. J., & Quinn, B. G. (1979). The determination of the order of an autoregression. *Journal of the Royal Statistical Society: Series B (Methodological)*, *41*(2), 190–195.

Hatemi-j, A. (2003). A new method to choose optimal lag order in stable and unstable VAR models. *Applied Economics Letters*, *10*(3), 135–137.

Hoover, K. D. (2005). Automatic inference of the contemporaneous causal order of a system of equations. *Econometric Theory*, *21*(1), 69–77.

Hosking, J. R. (1980). The multivariate Portmanteau statistic. *Journal of the American Statistical Association*, *75*(371), 602–608.

Huang, R. D., Masulis, R. W., & Stoll, H. R. (1996). Energy shocks and financial markets. *The Journal of Futures Markets (1986-1998)*, *16*(1), 1.

Jarque, C. M., & Bera, A. K. (1987). A test for normality of observations and regression residuals. *International Statistical Review/Revue Internationale de Statistique*, 163–172.

Ji, Q., Zhang, H.-Y., & Geng, J.-B. (2018). What drives natural gas prices in the United States? A directed acyclic graph approach. *Energy Economics*, *69*, 79–88.

Kalisch, M., Mächler, M., Colombo, D., Maathuis, M. H., & Bühlmann, P. (2012). Causal inference using graphical models with the R package pcalg. *Journal of Statistical Software*, *47*(11), 1–26.

Kilian, L., & Park, C. (2009). The impact of oil price shocks on the US stock market. *International Economic Review*, *50*(4), 1267–1287.

Kliesen, K. L., & Mill, J. S. (1994). The economics of natural disasters. *The Regional Economist*, *332*.

Levitin, A. J., & Wachter, S. M. (2011). Explaining the housing bubble. *Geo. LJ*, *100*, 1177.

Maghyereh, A. (2006). Oil price shocks and emerging stock markets: A generalized VAR approach. *Global Stock Markets and Portfolio Management* (pp. 55–68). Springer.

Maghyereh, A., & Awartani, B. (2016). Oil price uncertainty and equity returns: Evidence from oil importing and exporting countries in the MENA region. *Journal of Financial Economic Policy*.

Maghyereh, A. I., Awartani, B., & Bouri, E. (2016). The directional volatility connectedness between crude oil and equity markets: New evidence from implied volatility indexes. *Energy Economics*, *57*, 78–93.

Malik, F., & Hammoudeh, S. (2007). Shock and volatility transmission in the oil, US and Gulf equity markets. *International Review of Economics & Finance*, *16*(3), 357–368.

Masih, R., Peters, S., & De Mello, L. (2011). Oil price volatility and stock price fluctuations in an emerging market: Evidence from South Korea. *Energy Economics*, *33*(5), 975–986.

Miller, J. I., & Ratti, R. A. (2009). Crude oil and stock markets: Stability, instability, and bubbles. *Energy Economics*, *31*(4), 559–568.

Obstfeld, M. (1994). Risk-taking, global diversification, and growth. *The American Economic Review*, *84*(5), 1310–1329.

Pan, X., Ai, B., Li, C., Pan, X., & Yan, Y. (2019). Dynamic relationship among environmental regulation, technological innovation and energy efficiency based on large scale provincial panel data in China. *Technological Forecasting and Social Change*, *144*, 428–435.

Pesaran, H. H., & Shin, Y. (1998). Generalized impulse response analysis in linear multivariate models. *Economics Letters*, *58*(1), 17–29.

Pfaff, B. et al. (2008). VAR, SVAR and SVEC models: Implementation within R package vars. *Journal of Statistical Software*, *27*(4), 1–32.

Prabhakaran, S. (2020). *Vector Autoregression (VAR) - Comprehensive Guide with Examples in Python*. Machine Learning Plus. https://www.machinelearningplus.com/time-series/vector-autoregression-examples-python/

R Core Team. (2021). *R: A language and environment for statistical computing*. R Foundation for Statistical Computing. Vienna, Austria. https://www.R-project.org/

Robinson, P. M. (1995). Log-periodogram regression of time series with long range dependence. *The Annals of Statistics*, 1048–1072.

Schwarz, G. (1978). Estimating the dimension of a model. *The Annals of Statistics*, *6*(2), 461–464.

Segal, G., Shaliastovich, I., & Yaron, A. (2015). Good and bad uncertainty: Macroeconomic and financial market implications. *Journal of Financial Economics*, *117*(2), 369–397.

Sims, C. A. (1980). Macroeconomics and reality. *Econometrica: Journal of the Econometric Society*, 1–48.

Souček, M., & Todorova, N. (2013). Realized volatility transmission between crude oil and equity futures markets: A multivariate HAR approach. *Energy Economics*, *40*, 586–597.

Spirling, A. (2007). 'Turning Points' in the Iraq Conflict: Reversible Jump Markov Chain Monte Carlo in Political Science. *The American Statistician*, *61*(4), 315–320.

Spirtes, P., Glymour, C., Scheines, R., et al. (2001). Causation, Prediction, and Search. *MIT Press Books*, *Second edition*, 84–89.

Swanson, N. R., & Granger, C. W. (1997). Impulse response functions based on a causal approach to residual orthogonalization in vector autoregressions. *Journal of the American Statistical Association*, *92*(437), 357–367.

Van Rossum, G., & Drake, F. L. (2020). *Python 3.9*. Python Software Foundation. Scotts Valley, CA. http://www.python.org

Wang, W. (2021). *Topic 3: Multivariate Time Series I.* [PDF slides]. Canvas. https://canvas.eur.nl/files/37396396/download?download_frd=1

Wang, X., & Wu, C. (2018). Asymmetric volatility spillovers between crude oil and international financial markets. *Energy Economics*, *74*, 592–604.

Wang, Y., Wu, C., & Yang, L. (2013). Oil price shocks and stock market activities: Evidence from oil-importing and oil-exporting countries. *Journal of Comparative Economics*, *41*(4), 1220–1239.

Wen, X., Wei, Y., & Huang, D. (2012). Measuring contagion between energy market and stock market during financial crisis: A copula approach. *Energy Economics*, *34*(5), 1435–1446.

Xu, W., Ma, F., Chen, W., & Zhang, B. (2019). Asymmetric volatility spillovers between oil and stock markets: Evidence from China and the United States. *Energy Economics*, *80*, 310–320.

Yang, Z., & Zhou, Y. (2017). Quantitative easing and volatility spillovers across countries and asset classes. *Management Science*, *63*(2), 333–354.

Zhang, D. (2017). Oil shocks and stock markets revisited: Measuring connectedness from a global perspective. *Energy Economics*, *62*, 323–333.

Appendices

A Code description

To obtain the results for this paper, I use the R (2021) software, its general statistical packages, additional packages (such as ‘pcalg’ and ‘vars’) and my own coding. The code consists of six different scripts: ‘Main’, ‘VARcode’, ‘VHARcode’, ‘Spillovers’, ‘VARspillovers’ and ‘VHARspillovers’. In ‘Main’ I install all necessary packages and import the realized semivariances and positive and negative semivariances series into R. Then, in ‘VARcode’ the VAR model is estimated from which the residuals are used to determine the DAGs using the ‘pcalg’ package. After that the DAG restrictions for the coefficient matrix of the SVAR representation are implemented and forecast error variance decompositions are calculated. Finally, the model diagnostics such as the white noise properties of the residuals are tested. The code for the VHAR model in the script ‘VHARcode’ is similar with the exception that I first calculate the weekly and monthly realized variances. The script ‘Spillovers’ provides four spillover functions, one for each model and based on an expanding as well a moving window. Note that for the reasons explained at the end of Section 4.5 only the expanding window spillover functions are used in this paper. The scripts ‘VARspillovers’ and ‘VHARspillovers’ call the spillover functions from ‘Spillovers’ to retrieve the spillover indices and plot the results.

In addition to the use of R, the Python software by Van Rossum and Drake (2020) is used to obtain the descriptive statistics in the file ‘DescriptiveStats’. The ADF test is performed by using Prabhakaran (2020).

B Information criteria

The BIC and HQ information criteria are given by the following equations

$$\mathrm{BIC}(m) = \ln[\det\widehat{\Sigma}_u(m)] + \frac{\ln T}{T} m K^2 \tag{21}$$

$$\mathrm{HQ}(m) = \ln[\det\widehat{\Sigma}_u(m)] + \frac{\ln\ln T}{T} m K^2 \tag{22}$$

where T is the sample size, m the lag order of the VAR process, K the dimension and $\widehat{\Sigma}_u$ the estimated covariance matrix of the VAR residuals. Table 8 presents the results of the selection criteria of the VAR processes up to lag 10.

Table 8

BIC and HQ values up to lag 10

	RV		*RS*$^-$		*RS*$^+$	
Lag	BIC	HQ	BIC	HQ	BIC	HQ
1	-9.372	-9.394	-7.844	-7.866	-8.405	-8.426
2	-9.721	-9.764	-8.165	-8.209	-8.749	-8.793
3	-9.845	-9.910	-8.297	-8.363	-8.887	-8.953
4	-9.891	-9.979	-8.357	-8.444	-8.951	-9.039
5	-9.916∗	-10.025	-8.389∗	-8.498	-8.971∗	-9.080
6	-9.891	-10.022	-8.375	-8.506	-8.956	-9.087
7	-9.877	-10.030∗	-8.364	-8.517	-8.942	-9.095
8	-9.850	-10.025	-8.344	-8.518∗	-8.921	-9.095∗
9	-9.819	-10.016	-8.315	-8.512	-8.887	-9.084
10	-9.800	-10.018	-8.290	-8.509	-8.866	-9.084

Note. The minimum value is indicated by an asterisk.

C VAR and VHAR residuals correlations

Tables 9 and 10 show the simple correlations between the negative and positive semivariances of the markets for both models. The rows correspond to the negative semivariances and the columns to the positive semivariances.

Table 9

VAR residual correlations between negative and positive semivariances

	N225	STO50	WTI	SPX
N225	0.099	0.141	0.026	0.111
STO50	-0.022	0.386	0.101	0.342
WTI	-0.011	0.060	0.883	0.144
SPX	-0.006	0.138	0.159	0.444

Table 10

VHAR residual correlations between negative and positive semivariances

	N225	STO50	WTI	SPX
N225	0.016	0.147	-0.002	0.106
STO50	-0.028	0.347	0.062	0.323
WTI	0.000	0.055	0.883	0.145
SPX	0.010	0.099	0.119	0.376

D VAR and VHAR model diagnostics

Figures 8, 9, 10 and 11 show the standardized residuals plots for the negative and positive semivariances of the VAR and VHAR models.

Figure 8

Standardized residual plots negative semivariances VAR model

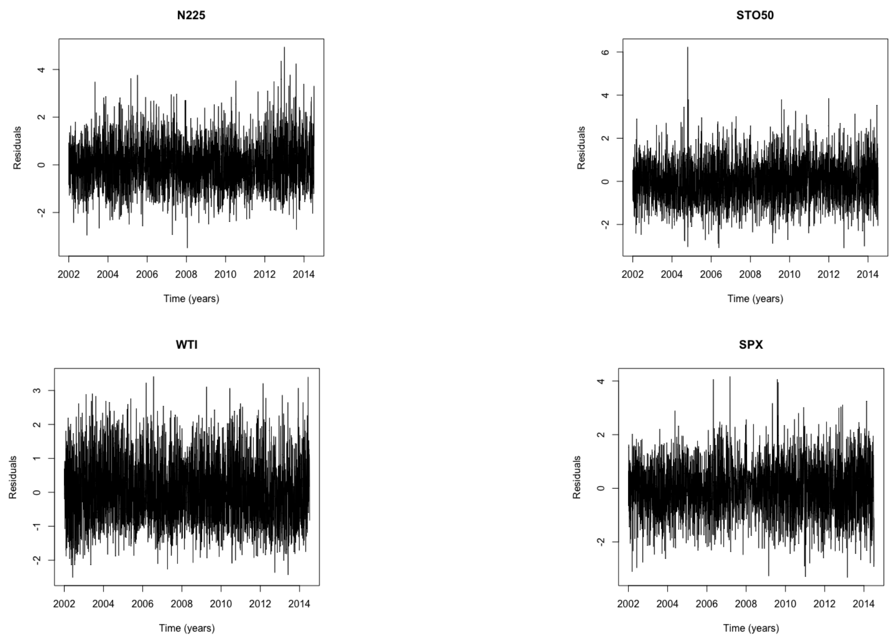

Figure 9

Standardized residual plots positive semivariances VAR model

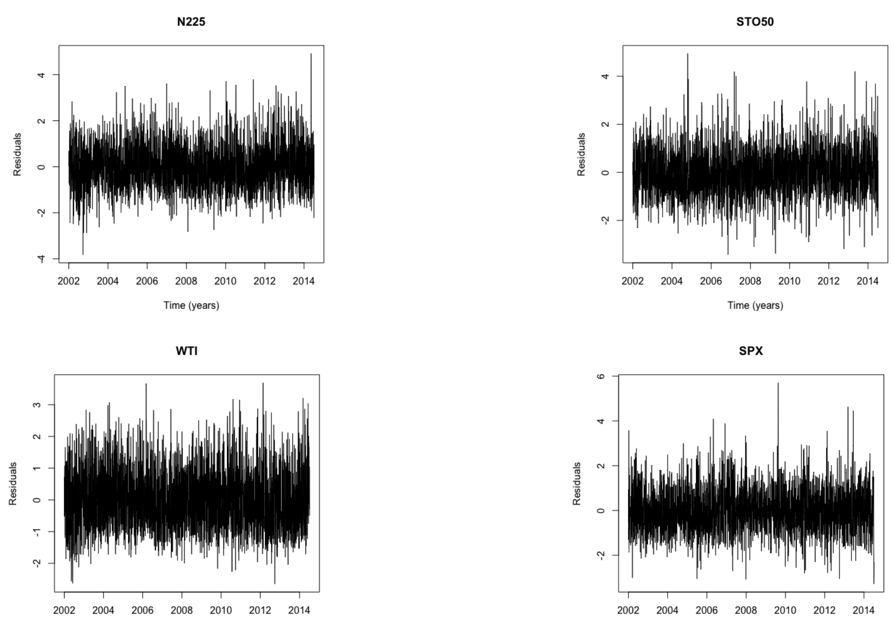

Figure 10

Standardized residual plots negative semivariances VHAR model

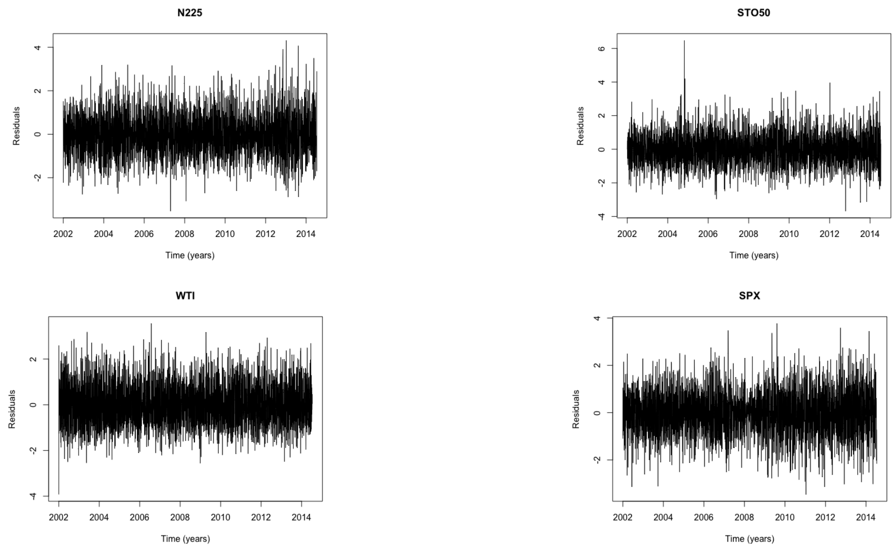

Figure 11

Standardized residual plots positive semivariances VHAR model

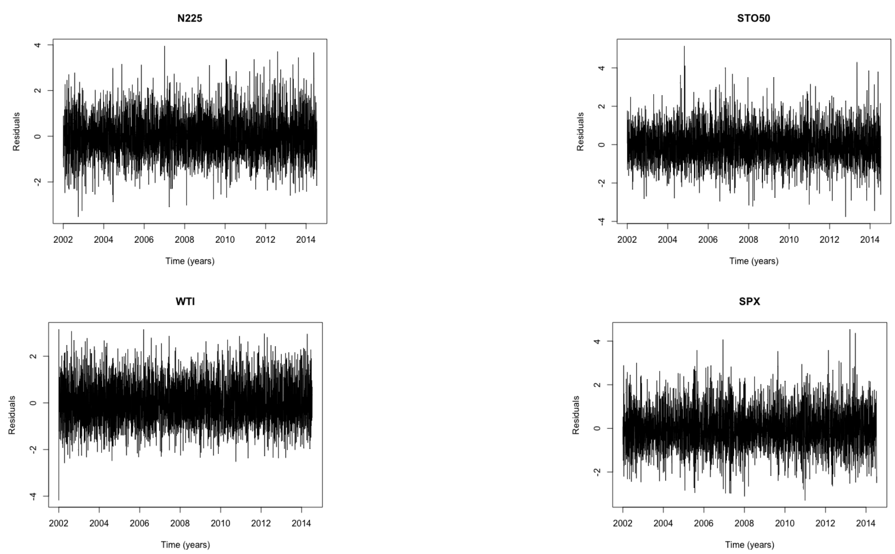

Figure 12 shows the robustness check for the total volatility spillover and total semivariances spillover for both models.

Figure 12

Robustness check spillover measures

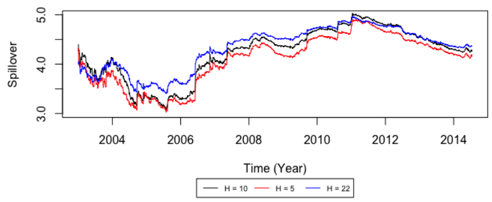

(a) *Total volatility spillover VAR*

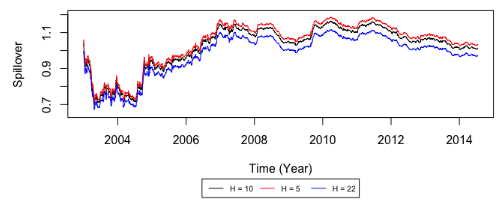

(b) *Total volatility spillover VHAR*

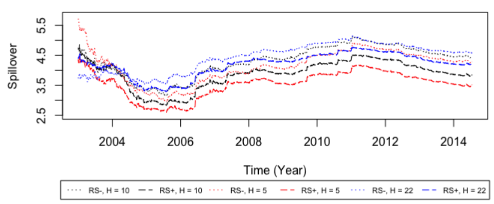

(c) *Total semivariances spillover VAR*

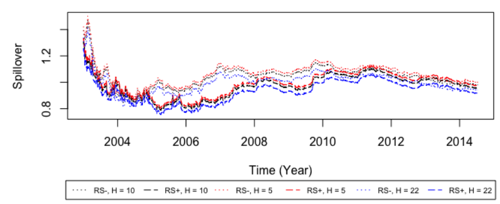

(d) *Total semivariances spillover VHAR*